Digital Finance (2024) 6:283–318
https://doi.org/10.1007/s42521-023-00103-y

ORIGINAL ARTICLE

Optimal trade execution in cryptocurrency markets

Nils Bundi[1] · **Ching-Lin Wei**[2] · **Khaldoun Khashanah**[3]

Received: 30 April 2023 / Accepted: 16 December 2023 / Published online: 24 January 2024
© The Author(s) 2024

Abstract

Novel technologies allow cryptocurrency exchanges to offer innovative services that set them apart from other exchanges. In this paper we study the distinct features of cryptocurrency fee schedules and the implications for optimal trade execution. We formulate an optimal execution strategy that minimizes the trading fees charged by the exchange. We further provide a proof for the existence of an optimal execution strategy for this type of fee schedule. The optimal strategy involves both market and limit orders on various price levels. The optimal order distribution scheme depends on the market conditions expressed in terms of the distribution of limit order execution probabilities and the exchange's specific configuration of the fee schedule. Our results indicate that a strategy kernel with an exponentially decaying allocation of trade volume to price levels further away from the best price provides superior performance and potential reduction of trade execution cost of more than 60%. The robustness of these results is confirmed in an empirical study. To our knowledge, this is the first study of optimal trade execution that takes into consideration the full fee schedule of exchanges in general.

Keywords Cryptocurrencies · Market microstructure · Limit order book · Maker taker market

Ching-Lin Wei and Khaldoun Khashanah contributed equally to this work.

✉ Nils Bundi
nils.bundi@gmail.com

Ching-Lin Wei
clwei@alumni.stevens.edu

Khaldoun Khashanah
kkhashan@stevens.edu

[1] School of Engineering, Zurich University of Applied Sciences, Technikumstrasse 7, 8400 Winterthur, Switzerland

[2] Shin Kong Life Insurance Co., Ltd, No. 66, Sec. 1, Zhongxiao W. Rd., Zhongzheng Dist., Taipei 10018, Taiwan

[3] School of Business, Stevens Institute of Technology, 1 Castle Point Terrace, Hoboken, NJ 07030, USA

JEL Classification D47 · G11 · G12 · G14

1 Introduction

Cryptocurrency markets have matured significantly over the past years and have seen increasing adoption by institutional investors recently. According to data reported by the online service Buy Bitcoin Worldwide, institutional investors held more than 7% of the total Bitcoin supply valued at some USD 70bn as per end of 2021 (Buy BitcoinWorldwide, 2021). While primarily crypto-native firms or technology companies gain direct cryptocurrency exposure, the rise of cryptocurrency ETFs and other derivatives demonstrates the wider economy's appetite for this new investment class. The backbone of this emerging industry are new cryptocurrency exchanges offering efficient, secure and regulatory-compliant markets. While these exchanges generally operate an electronic limit order book (LOB) similar to other exchanges, they have developed a number of innovative service offerings such as 24/7/365 trading and instantaneously adapting fee tiers. The latter is characterized by an asymmetric maker-taker fee schedule with rebates rewarding continuous trading activity. Thereby, other than with traditional exchanges, the applicable trading volume is updated instantaneously after every executed trade rather than at the end of the day as is practice among traditional exchanges. It is well understood that an exchange's fee schedule affects trading activity (Lin et al., 2019), trader's welfare (Colliard & Foucault, 2012), market efficiency (Black, 2022) and has an impact, in particular, on large traders (Panayides et al., 2017). Furthermore, Cimon (2021) finds that trading fee schedules affect the routing decision of brokers who execute trades on behalf of their clients. However, the latter is irrelevant in our context because traders generally interact directly with the exchange and are not intermediated by brokers on cryptocurrency markets (Brauneis et al., 2022). Thus, trading venues carefully design their fee schedule to optimize for some target such as to maximize market making activities (Euch et al., 2021). On the other hand, empirical evidence shows that trading costs can significantly impact a trading strategy's performance. For example, Edelen et al. (2013) show that for actively managed funds the trading cost on a per-unit basis can be up to 80 basis points (bps) with trade commissions amounting to 14 bps and price impact to a staggering 53 bps. Hence, for institutional clients allocating large trading volumes, the execution quality of an asset manager is an important decision factor (Ben-Rephael & Israelsen, 2017). Consequently, organizations trading large volumes operate sophisticated tools in order to minimize trading cost (Battalio et al., 2016) and execution risk (Kozhan & Tham, 2012; Tsoukalas et al., 2019).

In general, optimal trade execution is considered the problem of finding a strategy that executes a trade of a certain volume of an asset within a defined time period at a minimal cost (Bertsimas & Lo, 1998; Chen et al., 2018). Perold (1988) proposes to quantify the execution cost by a strategy's *implementation shortfall*, which includes trading fees, price impact and opportunity cost from unfilled limit orders. One stream of literature focuses on the sub-space of optimal execution

strategies if *implementation shortfall* is due to price impact only (Almgren, 2003; Almgren & Chris, 2000; Forsyth, 2011; Forsyth et al., 2009). Gatheral and Schied (2012) show that an analytical solution can be obtained when assuming that the execution price follows a geometric Brownian motion (GBM). By focusing on the execution price dynamics only, however, the dynamic properties of real-world LOBs themselves are neglected. Other studies thus let the LOB dynamically adjust (e.g. the speed of recovery of supply/demand after a trade) to executed trades as part of an execution strategy (Alfonsi et al., 2010; Obizhaeva & Wang, 2013; Siu et al., 2019; Tsoukalas et al., 2019). Furthermore, Kashyap (2020) splits the execution cost into market impact (price impact due to the executed trade) and market timing (price movement due to other traders during the trade duration) and suggests a stochastic dynamic programming approach to solve numerically for optimal execution strategies.

A second stream of literature accounts for static trading fees as another component of a strategy's *implementation shortfall*. For instance, Guo et al. (2017) study optimal order placement strategies under an asymmetric maker-taker fee structure. Cont and Kukanov (2017) investigate an optimal routing policy of order placements in which fee schedules are allowed to differ for different trading venues. In a more recent study Schnaubelt (2021) applies a reinforcement learning approach to optimal trade execution under a static fee schedule and finds that the optimal execution strategy consists of both market and limit orders. Schnaubelt's results suggest that the optimal strategy allows for a reduction of the total execution cost by up to almost 37% compared to the immediate execution through market orders. While results generally confirm that, in the presence of maker-taker fee asymmetry, the optimal execution strategy involves both market and limit orders, often only limit orders at the best bid/ask price levels are analyzed. Further evidence suggests, however, that under certain market conditions (e.g. when the market price has a negative drift) the optimal execution strategy involves limiting orders deeper in the LOB (Figueroa-Lopez et al., 2018).

It is well understood that the asymmetry of maker-taker fee schedules has an important impact on a trade's *implementation shortfall* and, as a result, the behavior of traders on a given exchange. To our best knowledge, however, the problem of optimal trade execution under a fee schedule with volume rebates has not been studied so far (Jalal et al., 2021). In particular, in the context of the innovative features of fee schedules used by cryptocurrency exchanges, the volume rebate is an important dimension that may allow to further reduce the execution cost. Thus, this paper extends previous work on optimal trade execution in the presence of feature-rich fee schedules. The remainder of the paper is organized as follows. In Sect. 2 we formalize the LOB and its dynamics. An optimal trade execution strategy minimizing execution cost based on a trader's continuously updating fee rebates is developed in Sect. 3. Section 4 analyzes the properties of the optimal trade execution strategy on the basis of a stylized LOB and real-world fee schedule. We continue this analysis in Sect. 5 where the LOB model is now calibrated to empirical data of Kraken's Bitcoin/USD LOB. Section 6 concludes with a discussion of our results and an outlook to future research.

2 The limit order book

Modern trading venues rely on an electronic database where submitted limit orders are collected, ordered, and eventually matched and executed. The LOB can thus be represented by two queues $\mathbf{a}(t)$ and $\mathbf{b}(t)$ where ask (sell) and bid (buy) orders are organized according to their limit prices i and j;

$$\mathbf{a}(t) = (a_1(t), a_2(t), \dots, a_i(t), \dots, a_I(t)) \tag{1a}$$

$$\mathbf{b}(t) = (b_1(t), b_2(t), \dots, b_j(t), \dots, b_J(t)) \tag{1b}$$

Therein, $b_j(t)$ contains the total volume of all bid orders with price level j which have not been executed up to time t. Each price level is associated with a limit price $p_j^{(b)}(t)$ and available volume $v_j^{(b)}(t)$. Because the prices are ordered from highest with index $j = 1$ to lowest at index $j = J$, so that $p_1^{(b)}(t) > p_2^{(b)}(t) > \cdots > p_J^{(b)}(t)$. Similarly, let $b_0(t)$ denote a market buy order with associated price $p_0^{(b)(t)}$ and volume $v_0^{(b)}(t)$. A market order instruction to buy at the current market price can be expressed as an infinite bid price $p_0^{(b)}(t) = \infty$.

Order execution refers to the act of matching an incoming bid (ask) order with an appropriate number of ask (bid) orders from the LOB queue and updating the queue accordingly. In reality a number of factors can disturb the execution process, which are usually neglected in the literature.

Assumption 1 (Efficient LOB) *A number of common approximations to the LOB for an efficient order execution process are assumed here and applied throughout this model:*

- *Zero-latency of orders means the instantaneous submission of orders. Hence, orders submitted to the LOB arrive at observation time t.*
- *Complete information signifies no hidden liquidity in the LOB as observed by a trader.*
- *Long-term infinite LOB elasticity means that there is no permanent impact on market price due to orders of our trader. More specifically, placement and execution of our trader's orders do not permanently impact the composition of the LOB represented by* $\mathbf{a}(t)$ *and* $\mathbf{b}(t)$.

A more detailed discussion of these approximations can be found in Schnaubelt (2021). Based on Assumption 1, we can formalize the order execution process for an incoming ask order $a^*(t)$ and queued bid order $b_j(t)$.

Theorem 1 (Order execution) *Consider an LOB with bid queue* $\mathbf{b}(t)$ *observed at time t and a newly submitted ask order* $a^*(t)$ *with associated limit price* $p^*(t)$ *and volume* $v^*(t)$. *Let* $\bar{v}_j^{(b)}(t) = \sum_{l=1}^{j} v_l^{(b)}(t)$ *be the total volume in the bid queue up to price level j. Then, an order* $b_j(t)$ *in* $\mathbf{b}(t)$ *is completely executed if and only if*

1. $p^*(t) \leq p_j^{(b)}(t)$,
2. *and* $v^*(t) \geq \bar{v}_j^{(b)}(t)$

with orders $b_l(t), l = 1, \ldots, j$ *matched and executed sequentially.*

Proof The proof is straight forward and follows from the *price priority* rule and the assumption of only full-order executions. □

Theorem 1 implies that any ask order with limit price lower than the highest limit price in the bid queue (best bid) is immediately executed. It follows that $p_1^{(b)}(t) < p_1^{(a)}(t)$ at any time t where the difference $p_1^{(a)}(t) - p_1^{(b)}(t)$ is called the bid-ask spread and reflects the current mismatch between the seller and buyer prices on the market. Note that symmetric arguments hold for the ask queue $\mathbf{a}(t)$. However, the rest of the discussion centers on a large-order buying process. Thus, in order to simplify notation we suppress superscript (b) throughout the remainder of this work without confusion.

2.1 Cryptocurrency exchange fee schedule

As discussed previously cryptocurrency exchanges operate a maker-taker fee model similar to traditional exchanges (see e.g. Kraken (2021)). This model considers traders who submit limit orders which are added to the order queue $\mathbf{b}(t)$ as liquidity makers. Traders who submit orders that are immediately executed and thus remove orders (and their volume) from the queue are considered liquidity takers. Markets operating such a fee schedule are thus often referred to as maker-taker markets. In order to attract liquidity to the LOB maker-taker markets charge makers lower fees than takers. Furthermore, different fee tiers reward the accumulation of continuous trading volume with further fee rebates. A linear variant of this fee model can be stated in terms of a base fee $\eta \in \mathbb{R}^+$, maker rebate $a \in \mathbb{R}^+$, volume rebate $b \in \mathbb{R}^+$ and the following fee schedule;

$$f^+(v) = \eta - a - bv \tag{2a}$$

$$f^-(v) = \eta - bv \tag{2b}$$

where $f^+(v)$,$f^-(v)$ are the maker and taker fees based on the applicable cumulative trading volume v. This fee schedule thus allows for three distinct regimes as exposed in Fig. 1.

Note that in reality the volume rebate often follows a staircase function. For the purpose of this paper, a linear approximation seems to be reasonable.

While maker-taker fee schedules are common among traditional markets too, cryptocurrency exchanges have developed distinct features such as instantaneously updating fee tiers and thus continuously adapting volume rebates. This is in contrast to the practice among traditional exchanges where the applicable trading volume is updated discretely such as at the end of every trading day. As a result,

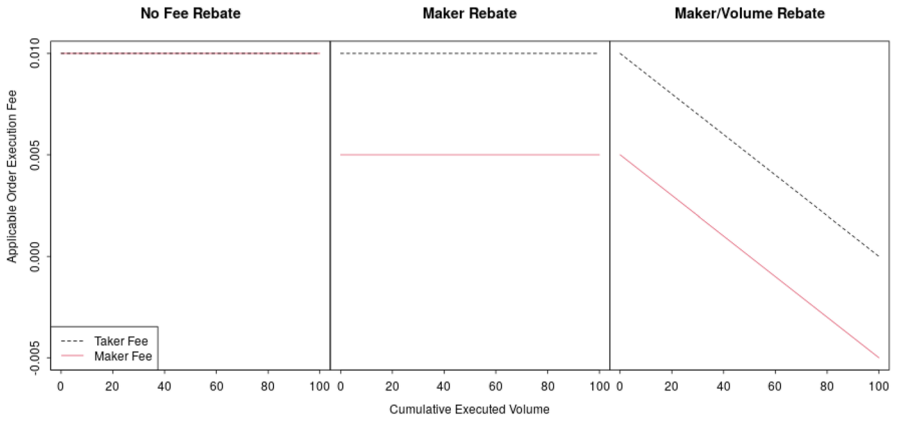


Fig. 1 Stylized fee schedule as found on cryptocurrency exchanges. The fee schedule is modelled by three parameters: a based fee η, maker rebate a for limit orders that are not immediately executed, and volume rebate b which is applied on the instantaneously updated cumulative trading volume

cryptocurrency traders are able to optimize an execution strategy for minimal trading fees on an intraday time scale.

2.2 Execution risk

Execution risk can have a significant impact on the performance of an execution strategy (Cheng et al., 2017). We thus take into consideration the uncertainty around the execution of a limit order placed in queue $\mathbf{b}(t)$ within the time horizon of the execution strategy. Therefore, we quantify the probability that a limit order $b_j(t)$ is executed within the defined time horizon. In fact, execution probabilities have been studied before but with a focus on limit orders at the best price level $j = 1$ (Cho & Nelling, 2000; Omura et al., 2000; Lo et al., 2002). We extend this research and develop a practical LOB model that allows us to quantify execution probabilities for limit orders on arbitrary price levels $j \in \{1, 2, \dots, J\}$. Therefore, for a given state of the LOB at time t, let $P_j^{(b)}(T|t)$ be the probability that the bid limit orders $b_j(t)$ are executed within the period $[t, t+T)$. For convenience we will simplify notation and write P_j. Theorem 1 indicates that this probability is driven by the arrival of ask orders with appropriate limit price $p^*(t)$ (necessary condition) and volume $v^*(t)$ (sufficient condition). Assuming a continuous order arrival process, one can model the dynamics of $(p^*(t), v^*(t))_{t\in[t,t+T)}$ as a 2-dimensional diffusion process. Continuous orderbook dynamics have been widely studied in literature and often the LOB mid-price $\frac{p_1^{(a)}(t)-p_1^{(b)}(t)}{2}$ is allowed to follow a diffusion process (Cheng et al., 2017; Guant et al., 2012; Huitema, 2014). Our model is inspired by the work of Yura et al. (2014) who find empirical evidence for correlated mid-price and volume changes and that this correlation is proportional to the distance of price level j to the best price. Based on these findings, we propose to model the process $(p^*(t), v^*(t))_{t\in[t,t+T)}$ as a bivariate (correlated) geometric Brownian motion.

Assumption 2 *Consider two independent Wiener processes $W_p(t)$ and $W_v(t)$ and let the dynamics of $(p^*(t), v^*(t))$ follow the bivariate geometric Brownian motion with drift terms μ_p, μ_v, volatilities σ_p, σ_v and correlation coefficient ρ in the variance-covariance matrix $\Sigma \cdot \Sigma'$*

$$\begin{bmatrix} d\ln(p^*(t)) \\ d\ln(v^*(t)) \end{bmatrix} = \begin{bmatrix} \mu_p \\ \mu_v \end{bmatrix} \mathrm{d}t + \Sigma \begin{bmatrix} dW_p(t) \\ dW_v(t) \end{bmatrix}$$

where $\Sigma \cdot \Sigma' = \begin{bmatrix} \sigma_p^2 & \rho\sigma_p\sigma_v \\ \rho\sigma_p\sigma_v & \sigma_v^2 \end{bmatrix}$.

We can now formulate the first passage times for the mid-price to fall below a certain limit bid price τ_p, and for the respective limit order volume to exceed the total limit order volume τ_v

$$\tau_p := \min_{t\geq 0}(t | p^*(t) \leq p_j^{(b)}(0)) \tag{3a}$$

$$\tau_v := \min_{t\geq 0}(t | v^*(t) \geq \bar{v}_j^{(b)}(0)). \tag{3b}$$

According to Theorem 1 the limit order execution probability P_j is the probability of both times τ_p and τ_v to be less than the trade period T, where τ_v will reflect a property that the probability is also subject to 'limit-order-book imbalance' (Kirchner & Vetter, 2020). In other words, we can write $P_j(T) = P(\tau_p \leq T \wedge \tau_v \leq T)$. Alternatively, utilizing the law of probability, we can also write

$$P_j(T) = P(\tau_p \leq T) + P(\tau_v \leq T) - P(\tau_p \leq T \vee \tau_v \leq T). \tag{4}$$

Applying the solution outlined in Section 2.2 in Zhou (2001), we can write the first two terms in Eq. (4) as follows[1]

$$P(\tau_p \leq T) = \Phi\left(-\frac{Z_p}{\sqrt{T}} - \frac{\mu_p}{\sigma_p}\sqrt{T}\right) + e^{-\frac{2\mu_p Z_p}{\sigma_p}}\Phi\left(-\frac{Z_p}{\sqrt{T}} + \frac{\mu_p}{\sigma_p}\sqrt{T}\right) \tag{5a}$$

$$P(\tau_v \leq T) = \Phi\left(-\frac{Z_v}{\sqrt{T}} - \frac{\mu_v}{\sigma_v}\sqrt{T}\right) + e^{-\frac{2\mu_v Z_v}{\sigma_v}}\Phi\left(-\frac{Z_v}{\sqrt{T}} + \frac{\mu_v}{\sigma_v}\sqrt{T}\right) \tag{5b}$$

with $Z_p = \frac{|ln(p^*(0)/p_j^{(b)}(0))|}{\sigma_p}$, $Z_v = \frac{|ln(v^*(0)/\bar{v}_j^{(b)}(0))|}{\sigma_v}$ and $\Phi(z)$ is the cumulative distribution function (cdf) of the standard normal distribution. Similarly, an analytical solution exists for the third term

[1] Note that Zhou in his original model has used a default threshold $C_i(t)$ which is dependent on time t reflecting firm i's debt position. Here, we fix the threshold defining the first passage times τ_p and τ_v to the bid order's limit price $p_j^{(b)}(0)$ and total volume placed $\bar{v}_j^{(b)}(0)$ which are constants. Hence, we have $\lambda_p = \lambda_v = 0$ and the expressions in Zhou (2001) simplify accordingly.

$$P(\tau_p \le T \vee \tau_v \le T) = 1 - \frac{2}{\alpha T} e^{a_1 x_1 + a_2 x_2 + a_T T} \sum_{n=1}^{\infty} \sin\left(\frac{n\pi\theta_0}{\alpha}\right) \cdot e^{-\frac{r_0^2}{2T}} \int_0^{\alpha} \sin\left(\frac{n\pi\theta}{\alpha}\right) g_n(\theta) \mathrm{d}\theta \tag{6}$$

with

$$\alpha = \begin{cases} \tan^{-1}\left(-\frac{\sqrt{1-\rho^2}}{\rho}\right) & \text{if } \rho < 0 \\ \pi + \tan^{-1}\left(-\frac{\sqrt{1-\rho^2}}{\rho}\right) & \text{otherwise} \end{cases}, \quad \theta_0 = \begin{cases} \tan^{-1}\left(\frac{Z_v\sqrt{1-\rho^2}}{Z_p - \rho Z_v}\right) & \text{if } (.) > 0 \\ \pi + \tan^{-1}\left(\frac{Z_v\sqrt{1-\rho^2}}{Z_p - \rho Z_v}\right) & \text{otherwise} \end{cases},$$

$$r_0 = Z_v / \sin(\theta_0), \qquad g_n(\theta) = \int_0^{\infty} r e^{-\frac{r^2}{2T}} e^{d_1 r \sin(\theta-\alpha) - d_2 r \cos(\theta-\alpha)} I_{\frac{n\phi}{\alpha}}\left(\frac{r r_0}{T}\right) \mathrm{d}r,$$

$$a_1 = -\frac{\mu_p\sigma_v - \mu_v\sigma_p\rho}{(1-\rho^2)\sigma_p^2\sigma_v}, \qquad a_2 = -\frac{\mu_v\sigma_p - \mu_p\sigma_v\rho}{(1-\rho^2)\sigma_v^2\sigma_p},$$

$$a_T = \frac{a_1^2\sigma_p^2}{2} + \rho a_1 a_2 \sigma_p \sigma_v + \frac{a_2^2\sigma_v^2}{2} + a_1\mu_p + a_2\mu_v,$$

$$d_1 = a_1\sigma_p + \rho a_2\sigma_v, \qquad d_2 = a_2\sigma_v\sqrt{1-\rho^2}$$

where I_ν is the modified Bessel function I with order ν.

From Eq. (4), it can be shown that $\frac{\partial P_j}{\partial T}$ is a valid probability density function with respect to the first passage time. Let $_{p_j(T) = \frac{\partial P_j}{\partial T}}$, then it follows that

$$p_j(T) = \frac{\partial P(\tau_p \le T)}{\partial T} + \frac{\partial P(\tau_v \le T)}{\partial T} - \frac{\partial P(\tau_p \le T \vee \tau_v \le T)}{\partial T} \tag{7}$$

As shown in Zhou (2001), all three terms in the above equation are non-negative functions. Since the law of probability suggests that $P(\tau_p \le T) + P(\tau_v \le T) > P(\tau_p \le T \vee \tau_v \le T)$ for all positive T, $p_j(T)$ is also a non-negative function. By integration, we have $_{P(\infty) = \int_0^{\infty} p_j(T)\mathrm{d}T = 1}$ and $P(T_1) - P(T_0) = \int_{T_0}^{T_1} p_j(T)\mathrm{d}T$ for any $T_1 > T_0$. Thus, $p_j(T)$ is a valid probability density function.

3 Optimal trade execution

The objective of optimal trade execution is to minimize the execution cost or, as previously discussed, the execution strategy's *implementation shortfall*. Therefore, the trader may split the trade into any desirable sub-units placed on the LOB as either market or limit orders with a desired strategy expiration. At the strategy's expiration the unfilled orders are withdrawn and the residual trade volume is executed. We consider a purely static setting where the trader does not dynamically adjust his orders once submitted. This is different from previous studies which generally find a dynamic execution strategy where orders are re-evaluated during the execution of the strategy (Almgren & Chris, 2000; Chen et al., 2018; Cont & Kukanov, 2017; Schnaubelt, 2021). Thus, our strategy is particularly useful for trade mandates with

a relatively short expiration T within which the shape of the LOB does not significantly change.

3.1 Trade execution strategy

Consider a mandate of trading N units of a certain asset against another asset within a fixed expiration T. The execution of that trade may involve any combination of maker and taker fees. We thus represent this trade as the triplet $(\mathbf{w}, N, T)$ with execution strategy $\mathbf{w} = (w_0, w_1, \dots, w_J)$ where elements w_j, $w_j \in \mathbb{R}^+ \forall j$ and $\sum_{j=0}^{J} w_j = 1$, reflect the proportional allocation of the total trade volume N to buy orders $b_j(t), j = 0, 1, \dots, J$. Note that, as defined above, $b_0(t)$ represents the submitted market buy order and $b_j(t), 0 < j \leq J$ the respective limit orders.

In the rest of the model, we focus on the special case where the strategy's *implementation shortfall* is defined purely by the trading fees due to the exchange fee schedule $(f^+(v), f^-(v))$. We thus neglect other types of execution costs such as price impact. This is in contrast to previous studies which have focused on the latter and excluded trading fees in their analyses. The fact that empirical evidence (Edelen et al., 2013; Schnaubelt, 2021) suggests a significant contribution of trading fees to overall execution cost motivates our assumption. Thus, the objective of strategy $\mathbf{w}$ is to minimize the trading fees associate with trade execution.

3.2 Trade execution

When submitted to the LOB, trade $(\mathbf{w}, N, T)$ is executed by the exchange according to Theorem 1. Specifically, the execution of the overall trade proceeds in the sequential execution of trade volume $w_j N$ allocated to orders b_j in queue $\mathbf{b}$ starting from the lowest and iterating to the highest price level. While orders are executed along this sequence cryptocurrency exchanges instantaneously update the accumulated trading volume v_j as outlined in Sect. 2.1. We can describe this updating process in terms of three steps as follows;

Step 1: At t, the market order with volume $w_0 N$ is executed immediately with an applicable rolling trading volume of v_0, which is the trader's initial trading volume accumulated prior to the submission of the trade.

Step 2: Within the period $[t, t+T)$, limit orders are executed sequentially and yield a new applicable rolling trading volume

$$v_j = v_{j-1} + \mathbf{I}_{j-1}(T) w_{j-1} N \quad \forall j = 1, 2, \dots, J+1 \tag{8}$$

where $\mathbf{I}_j(T)$ is an indicator function with $\mathbf{I}_j(T) = 1$ if the order at price level j is fully executed within $[t, t+T)$ and $\mathbf{I}_j(T) = 0$ otherwise.

Step 3: At $t+T$, an additional market order is placed and executed immediately covering the residual volume of the limit orders that were not executed

within trade period $[t, t+T)$. Hence, the volume of the residual order is $\sum_{j=1}^{J}(1-\mathbf{I}_j(T))w_jN$ with applicable rolling trading volume of v_{J+1} such that $\sum_{j=1}^{J}(1-\mathbf{I}_j(T))w_jN + v_{J+1} = N + v_0$.

Note that in Eq. (8) we assume that the applicable cumulative trading volume is updated after every executed trade. As discussed previously this reflects an innovative feature of cryptocurrency exchanges and allows for the execution strategy to realize respective fee rebates even if executed within an intraday period.

3.3 Trade execution cost

We are now in a position to express the trade execution cost in terms of the trade $(\mathbf{w}, N, T)$ and initial trade volume v_0. Therefore, we simply accumulate the fees applied when sequentially executing the orders placed in the LOB according to strategy $\mathbf{w}$. We can write this as follows

$$c(\mathbf{w}, N, T) = f^{-}(v_0)w_0N + \sum_{j=1}^{J} f^{+}(v_j)\mathbf{I}_j(T)w_jN + f^{-}(v_{J+1})\sum_{j=1}^{J}(1-\mathbf{I}_j(T))w_jN \quad (9)$$

We can write the distribution of the indicator $\mathbf{I}_j(T)$ as follows;

$$\mathbf{I}_0(T) = 1 \quad \text{with probability } 1 \quad (10a)$$

$$\mathbf{I}_j(T) = \begin{cases} 1 & \text{with probability } P_j(T) \\ 0 & \text{with probability } 1 - P_j(T) \end{cases}, j = 1, \ldots, J. \quad (10b)$$

with order execution probabilities $P_j(T)$ defined in Eq. (4). Probability $P\big(\mathbf{I}_0(T) = 1\big) = 1$ can be inferred from Assumption 1 which says that an efficient LOB allows for the immediate execution of market orders. Furthermore, the assumption also suggests LOB elasticity such that the execution of a trade does not materially affect the structure of the LOB and, hence, the implied execution probabilities. As a result, we are able to compute the expected trade execution cost from Eq. (9) by substituting the indicator functions with the respective execution probabilities

$$\begin{aligned} E[c(\mathbf{w}, N, T)] =& f^{-}(v_0)w_0N + \sum_{j=1}^{J} f^{+}(E[v_j])P_j(T)w_jN \\ &+ f^{-}(E[v_{J+1}])\sum_{j=1}^{J}(1-P_j(T))w_jN \end{aligned} \quad (11)$$

$$\min_{\mathbf{w}} E[c(\mathbf{w}, N, T)] \quad (12)$$

Optimizing over the strategy vector $\mathbf{w}$ results in a $J+1$ dimensional optimization problem. Especially for strategies involving a large number of price levels J this may

be challenging to solve in reality. We thus resort to a more robust approach in the next section.

3.4 Strategy kernels

In general, the existence and uniqueness of optimal solutions to the high-dimensional problem depend on the corresponding Hessian matrix and its eigenvalues. Exploring the linear-algebraic cases of minima, maxima, or saddle points can obscure the purpose of this paper while not adding much value to the learned reader. On the other hand, we show that solving Eq. (12) with a strategy kernel ensures that the second-order condition in Hessian matrix is satisfied to obtain an optimal solution while the kernel distributes the volume of the J limit orders according to the kernel of choice. Thus, a more practical approach is to operate along a narrower class of trading strategies that reduces the dimension of the optimization problem (Brown & Smith, 2011). Therefore, we propose a distinct class of trade execution strategies to reduce the dimension of the optimal execution strategy problem. The specific form of execution strategies proposed is as follows;

$$w_j = \begin{cases} 1-\gamma, & \text{if} \quad j = 0 \\ \gamma K_j, & \text{else} \end{cases} \tag{13}$$

with strategy kernel $K_j \in (0,1)$ and $\sum_{j=1}^{J} K_j = 1$. The execution strategy is then fully defined by $\gamma \in (0,1)$ and expresses the trader's allocation of the total trade size N to limit orders. On the other hand, the strategy kernel K_j defines how this allocation is split into smaller limit orders and distributed over price levels j. While the strategy kernel can take any shape, three intuitive choices are proposed here

$$\text{Constant} \quad K_j = \frac{1}{J} \tag{14a}$$

$$\text{Linear} \quad K_j = \frac{J-j}{\sum_i J-i} \tag{14b}$$

$$\text{Exponential} \quad K_j = \frac{e^{-\alpha j/J}}{\sum_i e^{-\alpha i/J}} \tag{14c}$$

As a result, utilizing a strategy kernel allows us to reduce the problem of finding an optimal execution strategy to a one-dimensional optimization problem of the form

$$\min_{\boldsymbol{\gamma}} E[c(\gamma, N, T)] \tag{15}$$

with

$$
\begin{aligned}
E[c(\gamma, N, T)] &= N(\eta - bv) - N\left(bN + a\sum_{j=1}^{J} P_j(T)K_j\right)\gamma \\
&+ bN^2\left(1 - \sum_{i=1}^{J} P_i(T)K_i + \sum_{j=1}^{J}\left(\sum_{i=j}^{J} P_i(T)K_i\right)P_j(T)K_j\right)\gamma^2
\end{aligned}
\tag{16}
$$

A proof of Eq. (16) can be found in Appendix A.

Based on this result, we can formulate the following Theorem that provides a condition on the existence of a solution to the optimization problem presented above and, thus, an optimal trade execution strategy.

Theorem 2 (Optimal execution strategy) *For a given J and T, the expected total execution cost* $E[c(\gamma, N, T)] = c_0 - c_1(T)\gamma + c_2(T)\gamma^2$ *with* $c_0 = N(\eta - bv_0)$, $c_1(T) = N[Nb + ag(T)]$, $c_2(T) = N^2 bh(T)$, $g(T) = \sum_{j=1}^{J} P_j(T)K_j$, *and* $h(T) = 1 - \sum_{i=1}^{J} P_i(T)K_i + \sum_{j=1}^{J}\left(\sum_{i=j}^{J} P_i(T)K_i\right)P_j(T)K_j$ *has a local minimum* $c^*(N,T) = c_0 - \frac{c_1(T)^2}{4c_2(T)}$ *for an optimal strategy* $\gamma(T)^* = \frac{c_1(T)}{2c_2(T)}$ *if and only if* $N > \frac{ag(T)}{[2\,h(T)-1]b}$ *and* $h(T) > 1/2$.

A proof of Theorem 2 is outlined in Appendix B.

4 An example: large bitcoin buy order on Kraken exchange

The goal of this section is to study the optimal trade execution strategy formulated in Theorem 2 on the basis of a real-world example. Specifically, we want to analyze the shape of the expected trade execution cost function $E[c(\gamma, N)]$ for different strategy kernels K_j and market regimes in terms of the distribution of order execution probabilities. Therefore, consider a buy trade of USD 10,000,000.00 worth of Bitcoin which should be executed at minimal cost within 60 min on Kraken Exchange.

Table 1 shows the trade parameters compiled by the mandated trader. Hypothetical numbers are chosen for the first four parameters T, N, J, and v_0 and all other parameters reflect the official fee schedule of Kraken Exchange (Kraken, 2021). In this stylized example, instead of calibrating the execution probabilities P_j to market data we will assume three distinct market regimes expressed in different, hypothetical, probability distributions $\tilde{P}_j(T)$; (1) uniform execution probabilities across the LOB, (2) execution probabilities decaying linearly with LOB depth, and (3) an exponential decay of the execution probabilities. More formally, we use the following market regimes in this example;

$$\text{Uniform} \quad \tilde{P}_j^u(T) = \xi \tag{17a}$$

$$\text{Linear Decay} \quad \tilde{P}_j^l(T) = \xi(J - (j-1))/J \tag{17b}$$

$$\text{Exponential Decay} \quad \tilde{P}_j^e(T) = \xi e^{-\zeta(j-1)/J}. \tag{17c}$$

Table 1 Kraken Exchange fee schedule parameters and parameters of a hypothetical Bitcoin buy trade worth USD 10,000,000 and with an execution target of 1 h

Parameter	Description	Value
T	Trade period	60 min
N	Total trade volume	10,000,000 USD
J	Available price levels	20
v_0	Initial trade volume	0
η	Taker fee	26 bps
a	Maker fee rebate	10 bps
b	Volume rebate rate	0.016 bps/USD 1 M
K_j	Strategy kernel	One of constant, linear or exponential
P_j	Market regime	One of uniform, linear or exponential

Hence, the market regimes all consider an execution probability of a limit order placed on the first price level of ξ but the probabilities behave differently on lower price levels. We calibrate the probability functions with $\xi = 0.4$, i.e. 40% execution probability within time T for the best bid order, and $\zeta = 10$ yielding a sharp exponential decay such that the linear and exponential decay regimes differ notably. Note that the assumption of uniform execution probabilities suggest that buy limit orders placed on different price levels all have the same probability, in this example 40%, of being executed against incoming sell orders. Theoretically, this is impossible as it implies that the first passage times τ_p and τ_v are equal across price levels i. Hence, the regime of uniform execution probabilities should be considered as a baseline scenario for comparison only.

The trader can now compute the minimal execution cost $c^*(N)$ according to Theorem 2. Figure 2 shows the expected trade execution cost for the three strategy kernels and the exponential decay market regime, $\tilde{P}^e_j(T)$. Execution strategy γ is represented by the x-axis and the resulting expected execution cost $E[c(\gamma, N)]$ is shown on the y-axis. For $\gamma = 0$, indicating execution as a large market order, the expected execution cost is USD 26,000 for all strategy kernels. This can easily be verified by applying the taker fee without maker and volume rebate to the total trade volume; $0.0026 * 10{,}000{,}000 = 26{,}000$. Furthermore, the optimal strategies γ^*(T) are indicated with a star-shaped marker for each kernel. The results suggest that the exponential strategy kernel yields the lowest minimal execution cost with a value of $c^*(\gamma^*, N) = 19{,}292$ for an optimal limit order allocation of $\gamma^*(T) = 0.73$ (rounded to 2 digits). Thus, the optimal strategy yields a significant potential cost reduction of about 26%.

We further want to understand the impact of the different market regimes on the optimal execution strategy. Figure 3 shows the optimal execution strategy γ^*(T) on the x-axis and the minimal execution cost $c^*(N, T)$ on the y-axis for all combinations of market regimes and strategy kernels. Points are plotted using the symbols 'o', 'Δ', and '+' for uniform, linear decay, and exponential decay market regimes while colors red, green, and blue indicate the constant, linear, and exponential kernels K_j. The following main observations are noteworthy; (1) the optimum for all

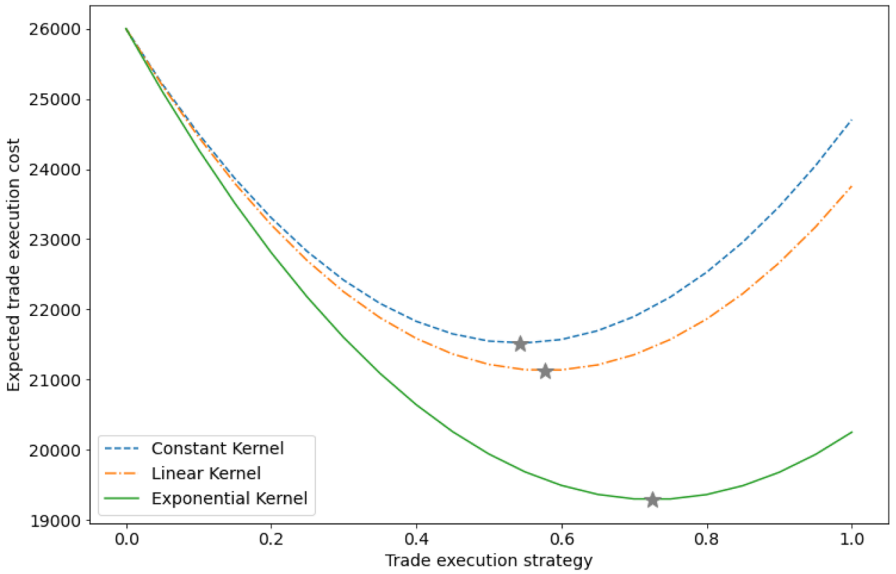


Fig. 2 Expected trade execution cost for different strategy kernels and exponentially decaying execution probabilities across the depth of a hypothetical Bitcoin/USD LOB. Minimal execution cost according to Theorem 2 are indicated with star-shaped markers

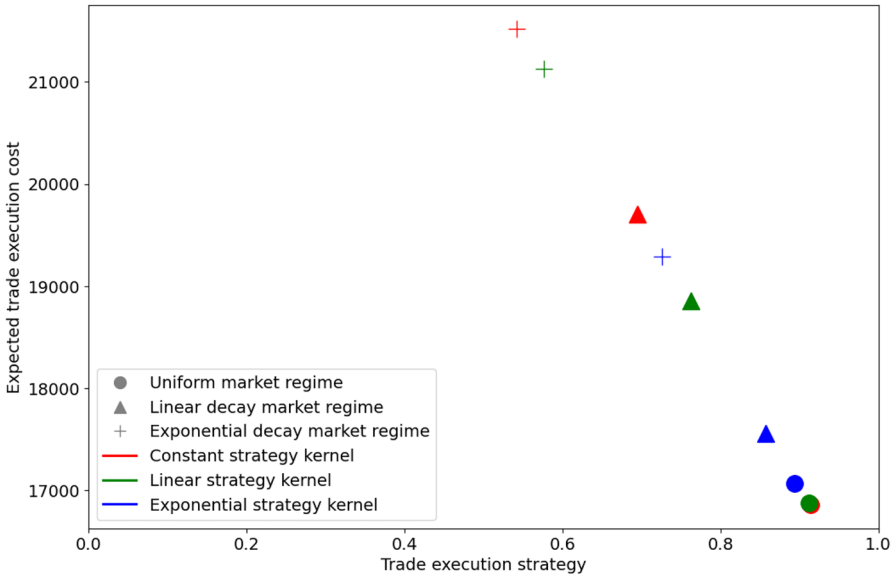


Fig. 3 Optimal trade execution strategy $\gamma^*(T)$ and minimal execution cost $c^*(N, T)$ for different strategy kernels and market regimes as reflected in the distribution of execution probabilities across the depth of a hypothetical Bitcoin/USD LOB

configurations requires the trader to allocate > 50% of her trade volume to limit orders, (2) the minimal execution cost is strongly correlated with the allocation of trade volume to limit orders, and (3) the minimal execution cost exhibits a strong negative correlation with execution probabilities $P_j(T)$ (higher execution probabilities result in lower minimal execution cost). Intuitively these results make sense as the fee rebates grow in the expected accumulated trade volume, $E[v_j]$, which itself increases along the execution path if a) the execution probabilities are higher and b) more volume is allocated to these limit orders. On the other hand, we observe that the exponential strategy kernel performs best for the exponential decay and linear decay market regimes but worst for the uniform regime. It is easy to see that this is due to the fact that terms g and h in Theorem 2 are maximized, and minimized respectively, if probabilities $P_j(T)$ and the kernel K_j exhibit a corresponding functional shape in price level j. As a result, the optimal choice of the strategy kernel, K_j, depends on the market regime or, in other words, on the shape of the LOB.

The overall minimal execution cost is USD 16,862 and is achieved in the uniform market regime and when applying the constant strategy kernel. This solution utilizes an execution strategy of $\gamma^*(T) = 0.91$ (rounded) suggesting that the trader should place 91% of the trade volume as limit orders allocated to the various price levels according to the constant kernel.

The results discussed in this section show that the expected execution cost of a large Bitcoin buy order can be reduced by up to 35% when optimizing for fee rebates only. This is a significant cost reduction potential improving the profitability of trading strategies and, thus, the performance of actively managed portfolios throughout the industry. In the following section, we will further expand on this analysis by estimating empirical order execution probabilities over different historical market regimes.

5 Empirical results

5.1 Bitcoin/USD data

We use historical LOB data for Kraken Exchange Bitcoin/USD market. Kraken Exchange is a major cryptocurrency exchange founded in 2011 and based in the US. According to different sources Kraken ranks among the largest cryptocurrency exchanges globally (Schnaubelt, 2021). Through their public APIs[2] we collected hourly LOB snapshots and the full history of intraday trade data (trade executions) spanning over almost 7.5 months (2021/5/1 to 2021/12/9). Due to a server outage data collection was interrupted for a number of days in July 2021 which results in a short data gap. Further, note that as discussed previously Kraken Exchange is open for trading on a 24/7/365 basis such that trading activity is reported at every day of the year. As a result, our sample consists of 5,224 LOB snapshots and 223 days of intraday trading activity. Based on this data we are able to reconstruct the complete

[2] A complete API documentation can be found here: https://docs.kraken.com/rest.

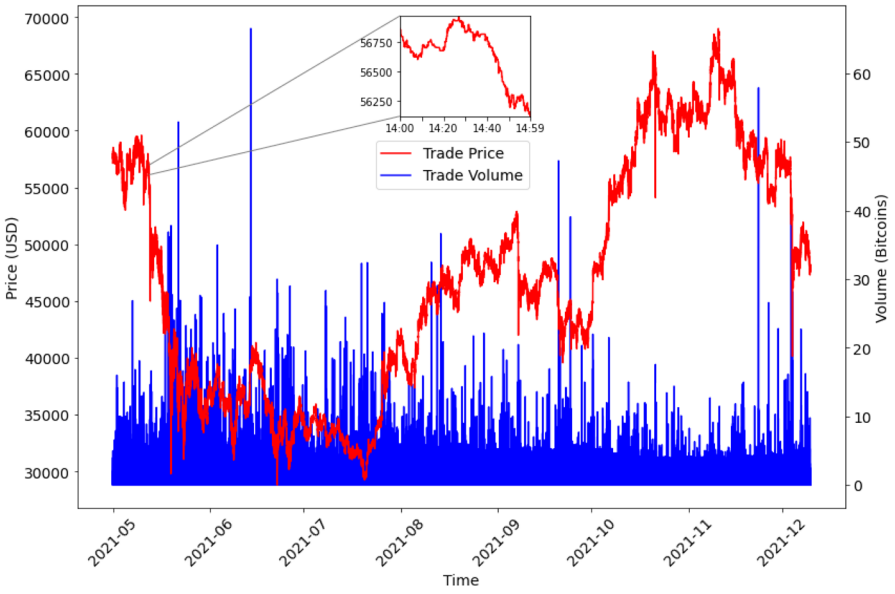


Fig. 4 Overview of the collected Bitcoin/USD intraday trade data. The sample spans a period of 223 trading days and contains observed execution prices (in red) and volume (in blue). A GBM calibration window of 1 h is shown for the LOB snapshot of 15:00 on May 12th 2021 (color figure online)

order queues $\mathbf{b}(t)$ and $\mathbf{a}(t)$ for all 5,224 snapshots. Our analysis shows that the empirical execution probabilities for limit orders beyond a certain price level becomes negligible (see Fig. 7). We thus limit the execution strategy to include only the first 300 price levels such that $J = 300$.

A summary of the collected intraday trade data is exhibited in Fig. 4. The data includes timestamp (x-axis), price (primary y-axis and red graph) and volume (secondary y-axis and blue bars) for all executed trades over the observation period. This data is exclusively used for calibrating our LOB model and the implied order execution probabilities. Figure 4 further shows the subsample of trade data used for the calibration of the execution probabilities for the UTC-15:00 LOB snapshot on May 12th 2021 in the zoom window. The methodology followed for the calibration is discussed in more detail in the following section.

5.2 LOB model calibration

The centerpiece of our LOB model is a bivariate geometric Brownian motion which represents the joint dynamics of the arriving ask price and volume. We approximate this process by the observed trade price $p(t)$ and volume $v(t)$. As discussed earlier, we thereby interpret market orders in the trade history as limit ask orders with a limit price of $-\infty$ such that we do not have to distinguish between trade executions from limit and market orders. Because trades are executed at random times t we first regularize the observed price and volume processes to

Table 2 Hypothesis testing for model parameters

Time period	Parameter	Estimated value	p-value
(2021-5-12 14:00:00, 2021-5-12 15:00:00)	μ_p	−3e−06	0.039
(2021-5-12 14:00:00, 2021-5-12 15:00:00)	μ_v	0.0004	0.988
(2021-5-12 14:00:00, 2021-5-12 15:00:00)	ρ	− 0.0444	0.007
(2021-05-01 02:00:00, 2021-12-09 23:59:59)	μ_p	−7e−09	0.858
(2021-05-01 02:00:00, 2021-12-09 23:59:59)	μ_v	−5e−08	0.999
(2021-05-01 02:00:00, 2021-12-09 23:59:59)	ρ	0.0217	< 1e−6

one-second frequency. Therefore, consider an equally-spaced time partition Π of the time interval $[0, t)$ and define $\Pi = \{[t_{i-1}, t_i)\}_{i=1}^{L}$ with $t_0 = 0$ and $t_L = t$. Here the length of each subinterval is equal to one second and the endpoint of the partition t corresponds to the snapshot time t so that $t_{i+1} - t_i = \frac{t}{L} = 1$. The partition Π allows us to derive a new, regular, price series $p_{i+1} = \max\{p(s)|s \in [t_i, t_{i+1})\}$ and volume series $v_{i+1} = \max\{v(s)|s \in [t_i, t_{i+1})\}$. Note that since we aggregate trade executions in 1000ms wide increments we are effectively remediating the problem of imprecise data from slow exchanges like Kraken as suggested by Foley et al. (2023). Using this regularized price and volume series data we are able to derive estimators $\hat{\mu}_p, \hat{\mu}_v, \hat{\sigma}_p, \hat{\sigma}_v, \hat{\rho}$ for the processes drift, volatility and correlation coefficients.[3] The regularized trade data, log-differences for price and volume and a scatter-plot of the two log-difference series are shown in Fig. 5 for the May 12th, 2021, 15:00 snapshot (i.e. the zoom window in Fig. 4). We see that both log-differences are stationary processes and, in other words, the drift terms $\hat{\mu}_p$ and $\hat{\mu}_v$ are negligible. Moreover, the price and volume log-differences seem only weakly correlated with a coefficient $\hat{\rho}$ close to zero. In order to verify this observation, we test the null hypotheses $\mu_p = 0$, $\mu_v = 0$, and $\rho = 0$ for different observation periods in Table 2. Since both the sample means and deviations (volatilities) are estimated quantities, we use a t-statistic to test the hypotheses above. The

[3] Specifically, we use the respective statistical moments of the regularized log-differences. These moments are computed as follows;

$$\hat{\sigma}_p = \sqrt{\frac{\sum_{s=-S+1}^{0}(\Delta ln(p_s) - \hat{\mu}_p)^2}{S-1}}$$

$$\hat{\sigma}_v = \sqrt{\frac{\sum_{s=-S+1}^{0}(\Delta ln(v_s) - \hat{\mu}_v)^2}{S-1}}$$

$$\hat{\rho} = \frac{\sum_{s=-S+1}^{0}(\Delta ln(p_s) - \hat{\mu}_p)(\Delta ln(v_s) - \hat{\mu}_v)}{\hat{\sigma}_p \hat{\sigma}_v}$$

with log-differences $\Delta ln(p_s) = ln(p_s) - ln(p_{s-1})$ and $\Delta ln(v_s) = ln(v_s) - ln(v_{s-1})$ and where $\hat{\mu}_p = \frac{\sum_{s=-S+1}^{0} \Delta ln(p_s)}{S-1}$, and $\hat{\mu}_v = \frac{\sum_{s=-S+1}^{0} \Delta ln(v_s)}{S-1}$.

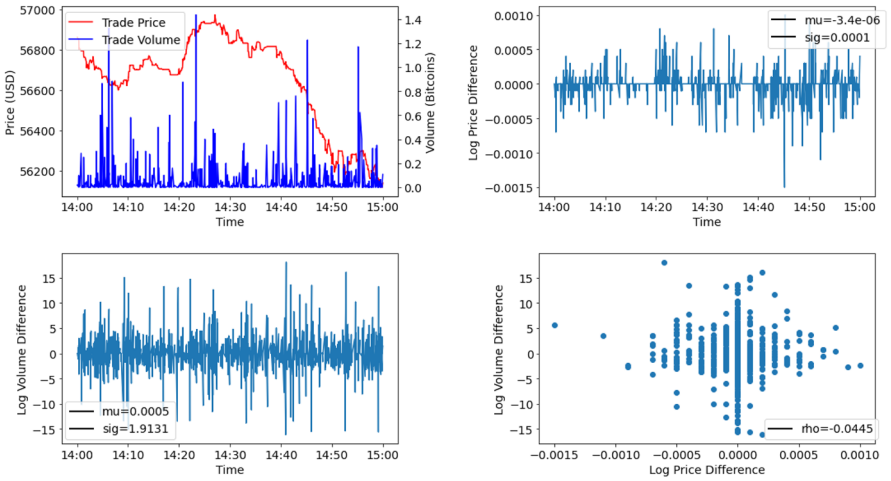


Fig. 5 Detailed view on the trade data used for calibrating the LOB model to the May 12th, 2021, 15:00 snapshot. Upper left: trade price and volume. Upper right: the log-differences for the trade price. Lower left: the log-differences for the trade volume. Lower right: scatter plot of the price log-differences vs volume log-differences

results in Table 2 suggest that the null hypotheses $\mu_p = 0$ and $\mu_v = 0$ cannot be rejected at the 1% significance level. This conclusion holds for the exhibited LOB snapshot sample as well as for the entire sample period. On the other hand, the null hypothesis $\rho = 0$ is rejected on the 1% significance level for both periods. Hence, we find statistical evidence that the price and volume processes indeed are correlated which is in line with the results of Yura et al. (2014).

Finally, it follows from the definition of partition Π that $p^*(t) = p_0$ and $v^*(t) = v_0$, i.e. the most recent submitted ask price and volume are given by the last trade price and volume on partition Π. This completes the calibration of our LOB model. The execution probabilities $P_j(t)$ are then obtained from the distribution of hitting times (3a) and (3b) as implied by limit prices $p_j^{(b)}(t)$ and cumulative buy volume $\bar{v}_j^{(b)}(t)$ which are observed on the respective LOB snapshot. These probabilities are computed using Eq. (4) and the model parameters obtained in this section. Thereby, using our hypothesis testing results presented in Table 2 and in particular the fact that we did not find statistical evidence for non-zero drift terms μ_p and μ_v, we can apply Zhou (2001)'s simplified form for Eqs. (5) and (6) (see Appendix D).

Figure 6 shows the buy order depth $\bar{v}_j^{(b)}(t)$ (green graph) and estimated execution probabilities (blue graph) for the same LOB snapshot again. The LOB model is calibrated with a partition window of $S = 3600$ s. The x-axis prints the buy price at levels $j \in (1, 2, \ldots, J)$, the respective buy order depth is shown on the primary y-axis (left hand side) and the resulting execution probability is printed on the secondary y-axis (right-hand side). As expected, the execution probability reaches a maximum of almost 1 for limit orders on the best price level and

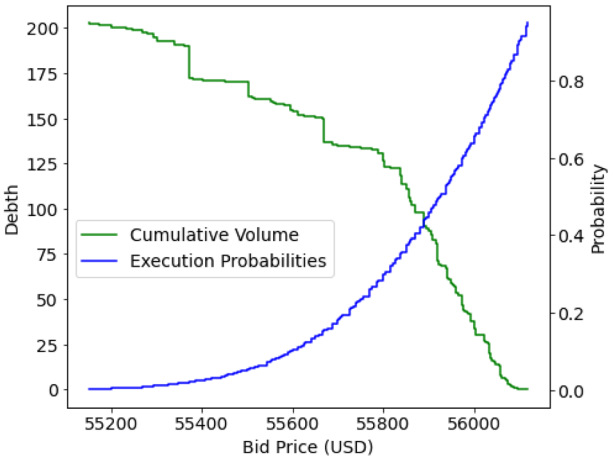


Fig. 6 Empirical buy order execution probabilities across the Kraken Exchange Bitcoin/USD LOB for the May 12th, 2021, 15:00 snapshot and a partition window of $S = 3600$ s

steadily decreases for orders deeper in the LOB. Thus, placing an order on lower price levels is associated with a higher risk of not being executed within the trade period T.

5.3 Snapshot analysis

We now calibrate the LOB model to the snapshots at the hours 12:00, 13:00, 14:00 and 15:00 on May 12th, 2021. Similar to Sect. 4 we then compute the optimal execution strategy and minimal execution cost for all the snapshots. Figure 7 reports the observed LOB order queue **b** (green line) and empirical execution probabilities (blue line) in the left column and the resulting optimal trade execution strategies for different strategy kernels in the right column. The graphs show that the shape of the order queue changes significantly over the course of the four snapshots. Specifically, the best bid price starts at about USD 56,500 in the 12:00 snapshot and increases to a maximal value of almost USD 57,000 2 h later. On the other hand, we also observe a significant adjustment of the LOB shape between 13:00 and 15:00. Since the LOB shape or the limit order queue **b**, respectively, has a direct impact on the limit order execution probabilities we also find this adjustment in the distribution of the execution probabilities between these same hours. Throughout the snapshots, the execution probabilities have a value of almost 1, for a limit buy order placed on the best price levels, and decrease monotonously to almost zero as the limit price decreases. Thereby, the rate of change of the execution probability is comparable across the sample. Yet, for the 14:00 snapshot the probability distribution exhibits a significantly longer tail indicating a large amount of low-volume low-price buy orders in the LOB.

The results for the optimal execution strategies confirm a maximal execution cost of $\eta N = \text{USD}26{,}000$ for a pure market order strategy, i.e. $\gamma = 0$, for all snapshots.

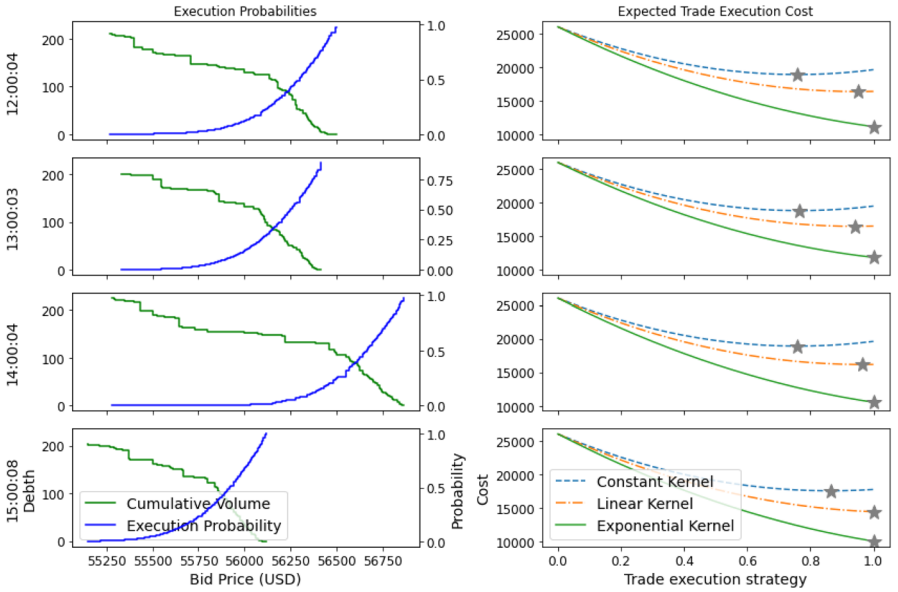


Fig. 7 LOB snapshot, empirical execution probabilities and resulting optimal trade execution strategy for different kernels and four Kraken Exchange Bitcoin/USD LOB snapshots taken on May 12th, 2021

In line with the results in Sect. 4 for all kernels the optimal strategy suggests a limit order allocation of more than 60%. For the 15:00 snapshot the optimal allocation reaches more than 80% for all strategy kernels. Further, we find that the exponential strategy kernel performs best throughout all snapshots with a limit order allocation of 100%. The exponential kernel is followed by the linear (second) and constant (third) kernels. This can be explained by the fact that the order execution probability distributions approximately follow an exponential function. Therefore, the exponential decay in trade volume allocation seems to most optimally deploy the limit orders in terms of the resulting fee rebate capture. The overall best result is achieved with the exponential kernel for the 15:00 snapshot where the execution cost can be reduced from USD 26,000 to 10,061 (rounded). This implies a cost reduction potential of about USD 15,939 or more than 60% on a USD 10 M trade.

5.4 Robustness

Previous results indicate that the exponential strategy kernel exhibits superior performance over the constant and linear kernels. We want to further test the robustness of this result over a longer trading period and, more importantly, different market regimes as discussed in Sect. 5.1. Therefore, we examine the optimal execution strategy for all 5,224 LOB snapshots over the full sample period which exhibits an annualized volatility of 97%, representative of the highly volatile Bitcoin market, and weeks with volatility spikes of up to 297%. The results

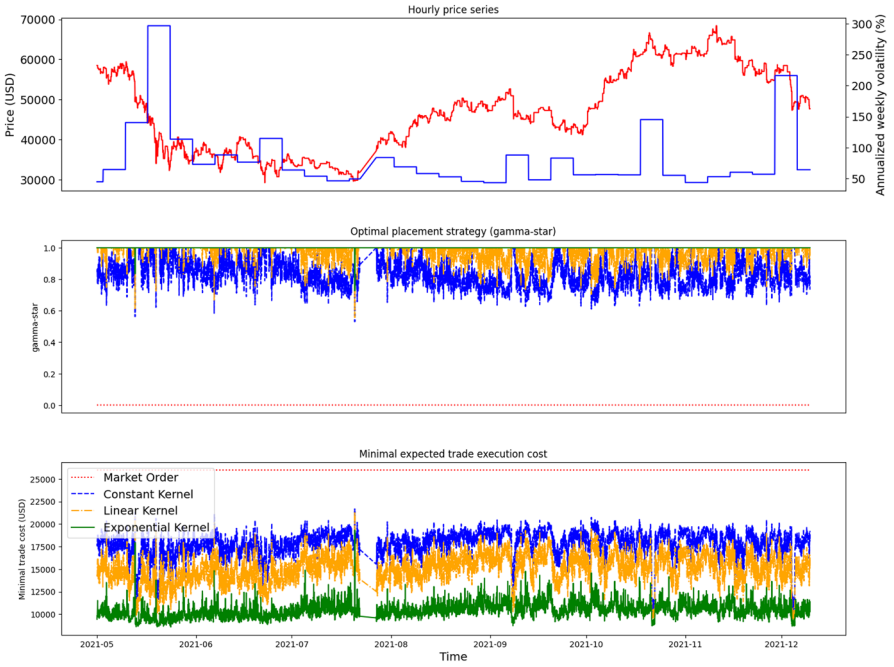


Fig. 8 Price and annualized volatility historical series (top figure), the optimal trade execution strategy (middle figure) and respective minimal execution cost (bottom figure) for different strategy kernels over a full sample of collected Bitcoin/USD LOB snapshots

Table 3 Mean and standard deviation of minimal trade execution cost for different strategy kernels over full sample of collected Bitcoin/USD LOB snapshots

Strategy	Mean	Standard deviation
Market order	26,000	0
Constant kernel	17,843	1406
Linear kernel	15,017	1561
Exponential kernel	10,465	846

of this analysis are shown in Fig. 8 where the optimal execution strategy $\gamma^*(T)$ for the three kernels is reported in the upper graph and the respective minimal execution cost in the lower graph. As a baseline the results for a pure market order strategy (i.e. $\gamma = 0$) is shown in red and, as expected, evaluates to constant execution cost of USD 26,000. The delta to the baseline results thus provides an estimation of a strategy's cost reduction potential over time. As indicated earlier due to an interruption in data collection a short gap in July can be observed in the graph for all strategies.

The results confirm a large allocation of order volume to limit orders leading to a significant cost reduction potential for all strategy kernels. Specifically, the

exponential strategy kernel suggests an optimal limit order allocation of 100% for almost all LOB snapshots. Table 3 reports the mean and standard deviation of the minimal execution cost over the sample period. These results indicate a mean cost reduction potential for the exponential kernel of $(26{,}000 - 10{,}465)/26{,}000 \approx 60\%$. At the same time, the constant and linear kernels not only result in a lower cost reduction but also higher uncertainty (in terms of standard deviation) associated with the reduction. Thus, these results confirm the superior performance of the exponential kernel and further indicate that this strategy also offers the most robust performance.

We further observe that these results are consistent across the sample period. Specifically, the general cost reduction potential and the superior performance of the exponential kernel are not affected by the different market regimes.

5.5 Sensitivity w.r.t. trade parameters

So far we have assumed that the parameters exposed in Table 1 are fixed and cannot be further optimized. This is meaningful assuming that the trader's mandate is to simply execute the trade $(\mathbf{w}, N, T)$. Weakening this assumption the trader may be in a position to suggest a more optimal trade configuration and specifically a more optimal size N or period T. Therefore, the trader may identify any critical points (N^*, T^*) on the minimal execution cost surface $c^*(N, T)$, where dependence on the trade period T has been included again, by requiring that its gradient $\nabla c^*(N,T) = \left(\frac{\partial c^*}{\partial N}, \frac{\partial c^*}{\partial T}\right)^\top$ evaluated at the critical point is the zero vector. We can thus establish the following system of equations

$$\nabla c^*(N^*, T^*) = \begin{pmatrix} (\eta - bv) - \frac{\lambda(N^*,T^*)}{2h(T^*)} \\ \frac{\lambda(N^*,T^*)}{4bh(T^*)^2}\left(\lambda(N^*,T^*)h'(T^*) - 2ag'(T^*)h(T^*)\right) \end{pmatrix} = \begin{pmatrix} 0 \\ 0 \end{pmatrix} \tag{18}$$

where we have substituted $\lambda(N, T) = Nb + ag(T)$ for convenience. As shown in Appendix E according to this methodology no critical point on the surface exists but these points exist only in the limit $T^* \to \infty$. Intuitively this makes sense as a larger trade period T^* leads to higher execution probabilities $P_j(T^*)$ and thus to more trade volume executed as limit orders at the various price levels. Because these limit orders accrue volume rebate and maker rebate, the minimal cost is expected to decrease.

These results are confirmed by the surface plot shown in Fig. 9 where the minimal execution cost is plotted as a function of the trade size N (x-axis) and trade period T (y-axis) for the 15:00:00 snapshot on May 12th, 2021. As a benchmark, the minimal cost for the fixed trade parameters as per Table 1 is indicated using a green star-shaped marker. Using these trade parameters and the exponential strategy kernel K_j the benchmark configuration results in an optimal strategy of $\gamma = 1$ and minimal expected execution cost of USD 9059 (rounded). We compute the results for the exponential strategy kernel only as this kernel has consistently shown the best performance. Figure 9 illustrates that the expected minimal execution cost decreases monotonously in the trade period T. Furthermore, the

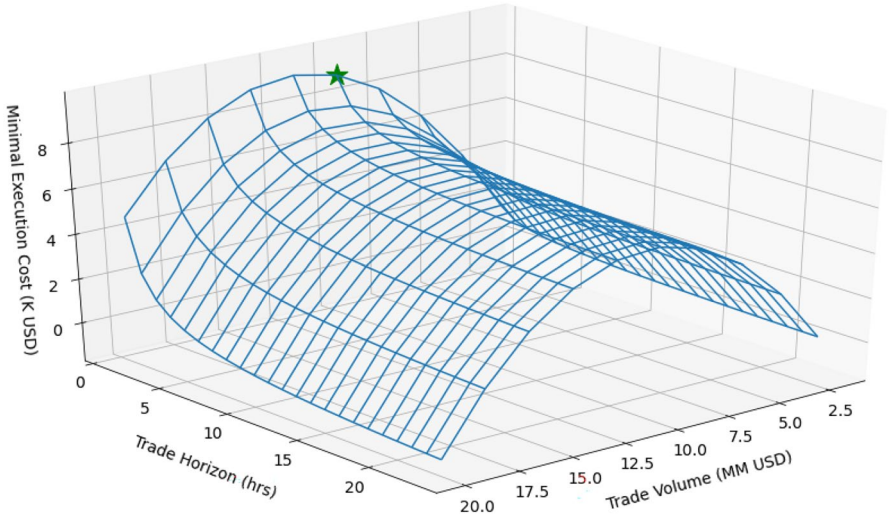


Fig. 9 Minimal trade execution cost as a function of the trade period and trade volume parameters. The result of the hypothetical Bitcoin buy trade is shown as a star-shaped marker

results show that the minimal cost follows a parabola-relationship with the trade size N. This is due to the nature of the fee schedule which applies a base fee η that is compensated by the rebate b with increasing trade volume and at a certain point the rebate starts dominating the base fee thus resulting in decreasing execution cost beyond that point. This result is confirmed by an analysis of Theorem 2 which reflects this parabola relationship in functional form. We conclude that to further optimize trade execution the trader should suggest to increase the trade period as much as possible.

5.6 Sensitivity w.r.t. exchange parameters

Trading venues stand in competition for liquidity and trading volume. Euch et al. (2021) show that the fee schedule expressed by rebates a, b is an important tool to attract trading activity. Specifically, the former study analyzes an optimal compensation scheme for market makers and the effect on trade execution cost on the respective exchange. Similarly, the fee schedule may be optimized for regular trader's execution cost. Therefore, consider the alternative representation $c^*_{N,T}(a,b)$ of function (C10) which expresses the minimal execution cost as a function of an exchange's fee rebates a, b and fixed trade parameters N, T as derived in Appendix C. In order to identify critical points (a^*, b^*) on this cost surface we again compute the gradient $\nabla c^*_{N,T}(a,b)$ and establish the system of equations by letting the gradient evaluate to zero in the critical points. As shown in Appendix F this criteria can be expressed as follows

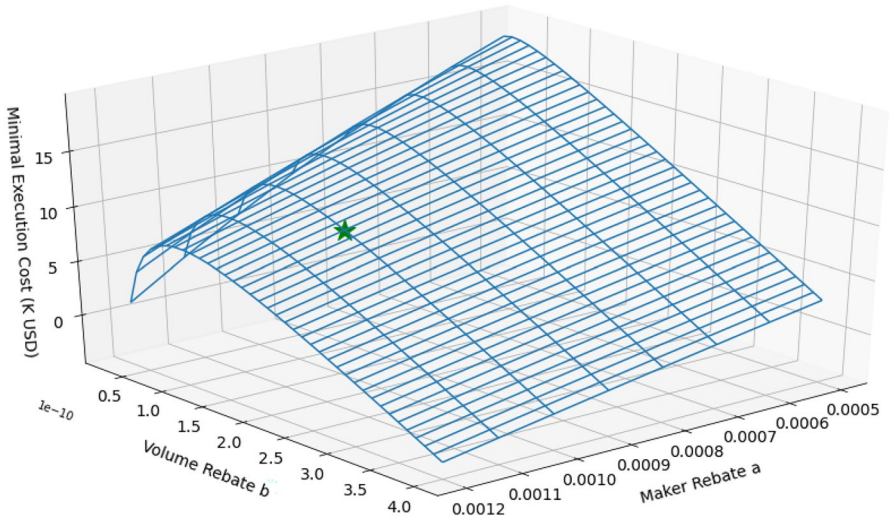


Fig. 10 Minimal trade execution cost as a function of the maker and volume fee rebate parameters. The result for the parameters observed on Kraken Exchange is shown as a star-shaped marker

$$\nabla c^*_{N,T}(a^*, b^*) = \begin{pmatrix} N + g(T)\frac{a^*}{b^*} \\ 4vh(T)N + N^2 - \left(g(T)\frac{a^*}{b^*}\right)^2 \end{pmatrix} = \begin{pmatrix} 0 \\ 0 \end{pmatrix} \tag{19}$$

The first equation reveals that, because all terms N, g, a, b are strictly positive, no solution exists and thus no critical point can be found. In fact, $c^*(a, b)$ is strictly decreasing in a which simply indicates that raising the maker rebate will decrease the expected cost reduction by placing more trading volume as limit orders irrespective of the specific strategy and execution probabilities. This can be seen in the expected execution cost, Function (16), where the maker rebate a is a strictly negative cost term. On the other hand, the relationship between the minimal execution cost and the volume rebate b turns out to be more complex. In fact, as expressed in Eq. (C11), the minimal execution cost is driven by two competing terms in the volume rebate b: for very small b the last term dominates while for large b the third term is the dominating term. Interestingly, for small volume rebates b the nominal volume rebate is driven by a differential of maker and volume rebate weighted by the expected relative executed limit order volume. In the case of a large volume rebate b, however, the nominal rebate increases as expected with the trade volume N.

We confirm these results in Fig. 10 which visualizes the minimal execution cost as a function of the exchange parameters. The green star-shaped marker indicates again the expected minimal execution cost when applying the hypothetical trade parameters from Table 1 as is used as a benchmark in Fig. 9 already. The graph reveals the strictly decreasing nature of the minimal execution cost in maker rebate a (x-axis). In contrast, we find a concave shape of the surface in volume rebate b (y-axis). We can derive a number of important implications for the operator of the trading venue. Essentially, for an operator seeking to attract loyal, large-volume

traders, the operator would optimize the fee schedule towards very small or large volume rebates both leading to lower execution cost. On the other hand, if the operator was to maximize the revenue from trading fees, she would be looking for a fee rebate configuration resulting in the max-min execution cost as per that surface.

6 Conclusions

Trade execution is subject to various cost components such as price impact or trading fees. In particular for large trades, the execution cost can significantly affect a trader's performance. The optimal execution strategy minimizes this cost by splitting the trade into smaller sub-units placed as market or limit orders with different bid/ask prices. We consider a setting where the exchange operates a maker-taker fee structure with additional fee rebates for cumulative trading volume. Specifically, the volume rebate is applied on a trade based on the instantaneously updated accumulated trading volume. This setting is motivated by the innovative fee schedules operated by emerging cryptocurrency exchanges like Kraken Exchange.

We show that for this fee schedule an optimal execution strategy exists and results in significantly lower trading fees compared to the baseline strategy which uses a single market order only. The optimal strategy consists of a combination of market and limit orders distributed over different price levels to maximize the applied volume rebates. Thereby, the specific order distribution scheme depends on the limit order execution probability distribution and thus on the market conditions when the trade is executed. However, we find that a strategy kernel with an exponentially decaying allocation of trade volume to limit prices generally provides the best performance. We test the robustness of these results in an empirical analysis based on a sample of 5,224 hly LOB snapshots across 223 trading days collected on Kraken Exchange. The results confirm the superior performance of the exponential strategy kernel over a constant and linear decay kernel. In fact, the exponential kernel suggests an allocation of trade volume to limit orders of 100% for almost all LOB snapshots and results in the highest cost reduction potential of sometimes more than 60%.

This work extends the existing body of literature in multiple ways. First the study confirms previous results on the significant impact of trade execution on the overall performance of actively managed trading strategies. Second, our results clearly point out the benefit of including limit orders beyond the best bid and ask prices in an order execution strategy.

An extension of this work would consider price impact as another component of a trade's execution cost. We expect two counteracting forces of price impact. The first negatively impacts the average buy price and is due to the executed market order. This effect is generally understood as an execution cost and has been analyzed extensively in previous studies. However, since the optimal execution strategy presented here splits a trade into any number of limit buy orders placed at decreasing buy prices a second force decreases the average buy price. Compared to the baseline strategy it is thus expected that our execution strategy is capable of further reducing a trade's execution cost. Further research may also be directed towards relaxing

some of the assumptions underpinning Theorems 1 and 2. In particular, supporting a multi-period strategy would allow for weakening the assumption of LOB elasticity and allow for the application of the strategy to markets with lower liquidity. Further, the dynamics of the joint volume and price process assumed in this work may be extended from a standard GBM to include richer features such as price jumps and stochastic volatility. This would allow the model to more accurately reflect the empirical features of crypto markets. Finally, while our model takes into account execution risk by applying the limit order execution probabilities on the different price levels, these probabilities have to be calibrated to LOB data first. Hence, the accuracy of these estimations has an important impact on the reliability of our model. Future research should be dedicated to analyzing this effect and the quantification of the strategy execution risk induced by the order execution probability estimation errors.

Appendix A: Proof for kernel-based trading cost function

Proof We will start by substituting linear fee functions $f^+(v), f^-(v)$ into Eq. (11). Further, for simplicity we will omit the expectation in the accumulated volume term and use the convention $v_j := E(v_j), j = 1, 2, \dots, J$ in the forthcoming of this proof. Hence, we can write the expected total trading cost as

$$
\begin{aligned}
E[c(\mathbf{w}, N, T)] &= N(\eta - bv_0)w_0 + N\sum_{j=1}^{J}(\eta - a - bv_j)P_j(T)w_j \\
&\quad + N(\eta - bv_{J+1})\sum_{j=1}^{J}(1 - P_j(T))w_j \\
&= N(\eta - bv_0)w_0 + (\eta - a)N\sum_{j=1}^{J}P_j(T)w_j \\
&\quad - bN\sum_{j=1}^{J}v_jP_j(T)w_j + \eta N\sum_{j=1}^{J}w_j \\
&\quad - \eta N\sum_{j=1}^{J}P_j(T)w_j - bNv_{J+1}\sum_{j=1}^{J}w_j + bN\sum_{j=1}^{J}v_{J+1}P_j(T)w_j \\
&= N(\eta - bv_0)w_0 + N\sum_{j=1}^{J}(\eta - aP_j(T))w_j + bN\sum_{j=1}^{J}(v_{J+1} - v_j)P_j(T)w_j \\
&\quad - bNv_{J+1}\sum_{j=1}^{J}w_j
\end{aligned}
\tag{A1}
$$

Plugging in the expressions for the accumulated volume $v_j = v + Nw_0 + N\sum_{i=1}^{j-1} P_i(T)w_i$ we can further simplify the expected total cost function

$$\begin{aligned}
E[c(\mathbf{w}, N, T)] &= N(\eta - bv)w_0 + N\sum_{j=1}^{J}(\eta - aP_j(T))w_j \\
&\quad + bN^2\sum_{j=1}^{J}\left(\sum_{i=1}^{J} P_i(T)w_i - \sum_{i=1}^{j-1} P_i(T)w_i\right)P_j(T)w_j \\
&\quad - bN\left(v + Nw_0 + N\sum_{i=1}^{J} P_i(T)w_i\right)\sum_{j=1}^{J} w_j \\
&= N(\eta - bv)w_0 + N\sum_{j=1}^{J}(\eta - bv - aP_j(T))w_j - bN^2 w_0\sum_{j=1}^{J} w_j \\
&\quad + bN^2\sum_{j=1}^{J}\left(\sum_{i=j}^{J} P_i(T)w_i\right)P_j(T)w_j - bN^2\sum_{i=1}^{J} P_i(T)w_i\sum_{j=1}^{J} w_j.
\end{aligned} \tag{A2}$$

Finally, replacing the strategy vector $\mathbf{w}$ with the strategy kernels the expected total trading cost can be rewritten as

$$\begin{aligned}
E[c(\gamma, N, T)] &= N(\eta - bv)(1-\gamma) + N\sum_{j=1}^{J}(\eta - bv - aP_j(T))K_j\gamma - bN^2(1-\gamma)\gamma\sum_{j=1}^{J} K_j \\
&\quad + bN^2\sum_{j=1}^{J}\left(\sum_{i=j}^{J} P_i(T)K_i\right)P_j(T)K_j\gamma^2 - bN^2\sum_{i=1}^{J} P_i(T)K_i\sum_{j=1}^{J} K_j\gamma^2 \\
&= N(\eta - bv) - N(\eta - bv)\gamma + N(\eta - bv)\gamma - aN\sum_{j=1}^{J} P_j(T)K_j\gamma \\
&\quad - bN^2\gamma + bN^2\gamma^2 + bN^2\sum_{j=1}^{J}\left(\sum_{i=j}^{J} P_i(T)K_i\right)P_j(T)K_j\gamma^2 \\
&\quad - bN^2\sum_{i=1}^{J} P_i(T)K_i\gamma^2 \\
&= N(\eta - bv) - N\left(bN + a\sum_{j=1}^{J} P_j(T)K_j\right)\gamma \\
&\quad + bN^2\left(1 - \sum_{i=1}^{J} P_i(T)K_i + \sum_{j=1}^{J}\left(\sum_{i=j}^{J} P_i(T)K_i\right)P_j(T)K_j\right)\gamma^2.
\end{aligned} \tag{A3}$$

□

Appendix B: Proof of Theorem 2

Proof The optimal γ will satisfy the following first and second order conditions.

$$\frac{\partial E[c(\gamma, N, T)]}{\partial \gamma} = 0 \tag{B4a}$$

$$\frac{\partial^2 E[c(\gamma, N, T)]}{\partial \gamma^2} > 0. \tag{B4b}$$

Since $E[c(\gamma, N, T)]$ is a quadratic function in γ, it can be expressed by

$$f(\gamma) = c_0 - c_1\gamma + c_2\gamma^2, \tag{B5}$$

where

$$c_0 = N(\eta - bv) > 0 \tag{B6a}$$

$$c_1 = N[Nb + ag(T)] > 0 \tag{B6b}$$

$$c_2 = bN^2 h(T) > 0 \tag{B6c}$$

$$g(T) = \sum_{j=1}^{J} P_j(T)K_j > 0 \tag{B6d}$$

$$h(T) = 1 - \sum_{i=1}^{J} P_i(T)K_i + \sum_{j=1}^{J}\left(\sum_{i=j}^{J} P_i(T)K_i\right)P_j(T)K_j > 0. \tag{B6e}$$

Note that $0 \leq \sum_{i=1}^{J} P_i(T)K_i < 1$ because $0 \leq P_i(T) \leq 1, \forall i$ by definition of a probability which leads to the inequalities above. As a result, we have

$$\frac{\partial E[c(\gamma, N, T)]}{\partial \gamma} = f'(\gamma) = 2c_2\gamma - c_1 \tag{B7a}$$

$$\frac{\partial^2 E[c(\gamma, N, T)]}{\partial \gamma^2} = f''(\gamma) = 2c_2 > 0 \tag{B7b}$$

Thus, by setting $f'(\gamma) = 0$ the local optimum $\gamma^*(T)$ evaluates to

$$\gamma * (T) = \frac{c_1}{2c_2} = \frac{Nb + ag(T)}{2bNh(T)} \tag{B8}$$

Furthermore, since $f''(\gamma) > 0$, $E[c(\gamma, N, T)]$ is a convex function in γ and $\gamma^*(T)$ is a local minimum.

Finally, we show that for $\gamma^*(T) \in (0,1)$, i.e. the minimum is found on the domain of γ, the condition $N > \frac{ag(T)}{[2h(T)-1]b}$ must be fulfilled. Therefore we first note that because $c_1 \geq 0$ and $c_2 > 0$ it follows that $\gamma^*(T) = \frac{c_1}{2c_2} \geq 0$. To prove that $\gamma^*(T) \leq 1$ we proceed as follows with an assumption that $h(T) > 1/2$

$$\begin{aligned}
\gamma^*(T) < 1 &\iff c_1 < 2c_2 \\
&\iff 2c_2 - c_1 > 0 \\
&\iff 2bh(T)N^2 - N[Nb + ag(T)] > 0 \\
&\iff 2bh(T)N - bN - ag(T) > 0 \\
&\iff [2h(T) - 1]bN > ag(T) \\
&\iff N > \frac{ag(T)}{[2h(T) - 1]b}.
\end{aligned} \tag{B9}$$

When $h(T) < 1/2$, we have $[2h(T) - 1]bN < ag(T)$, and thus $\gamma^*(T) > 1$ will be obtained. □

Appendix C: Derivation of the minimal expected execution cost functions

To derive the minimal expected execution cost as a function of the trade parameters we simply plug in the optimal execution strategy $\gamma^*(T)$ according to Theorem 2 into the minimal expected execution cost function $E[c(\gamma, N, T)]$;

$$\begin{aligned}
c^*(N,T) &= c_0 - c_1\gamma^*(T) + c_2(\gamma^*(T))^2 \\
&= c_0 - c_1\left(\frac{c_1}{2c_2}\right) + c_2\left(\frac{c_1}{2c_2}\right)^2 \\
&= c_0 - \frac{c_1^2}{2c_2} + \frac{c_1^2}{4c_2} \\
&= c_0 - \frac{c_1^2}{4c_2} \\
&= N(\eta - bv) - \frac{N^2[Nb + ag(T)]^2}{4bN^2h(T)} \\
&= N(\eta - bv) - \frac{[Nb + ag(T)]^2}{4bh(T)}
\end{aligned} \tag{C10}$$

Similarly, we can fix the trade parameters N, T and find the minimal expected execution cost as a function of an exchange's fee schedule or rebate parameters a, b, respectively. Using Eq. (C10) we can easily find this relationship by

$$
\begin{aligned}
c^*_{N,T}(a,b) &= N(\eta - bv) - \frac{[Nb + ag(T)]^2}{4bh(T)} \\
&= N\eta - \frac{Ng(T)}{2h(T)}a - \frac{N^2 b}{4h(T)} - Nvb - \frac{g(T)^2}{4h(T)}\frac{a^2}{b} \\
&= N\eta - \frac{Ng(T)}{2h(T)}a - \frac{4vh(T)N + N^2}{4h(T)}b - \frac{g(T)^2}{4h(T)}\frac{a^2}{b}.
\end{aligned}
\tag{C11}
$$

Appendix D: Simplified execution probability function

Zhou (2001) outlines in Section 2.1 his *Main Result 1* which is based on the assumption that the growth rate of the boundary value (in Zhou's model a firm's debt) and the process's drift term (firm's asset value in Zhou's model) are equal. However, in this work the boundary values defining first passage times τ_p and τ_v are the limit price $p_j^{(b)}(0)$ and cumulative buy volume $\bar{v}_j^{(b)}(0)$ which are constants. As discussed earlier we thus assume a zero growth rate of the boundary value. On the other hand, in Sect. 5.2 we find no statistical evidence for non-zero drift parameters μ_p and μ_v. As a result, for the purpose of our work we can make use of Zhou's assumption of equal boundary growth rate and process drift term and therefore utilize his *Main Result 1*. This allows us to write Eq. (5) in simplified form

$$
P(\tau_p \le T) = 2 * N\left(-\frac{Z_p}{\sqrt{T}}\right) \tag{D12a}
$$

$$
P(\tau_v \le T) = 2 * N\left(-\frac{Z_v}{\sqrt{T}}\right). \tag{D12b}
$$

Similarly, we can rewrite Eq. (6)

$$
\begin{aligned}
P(\tau_p \le T \vee \tau_v \le T) = 1 - \frac{2r_0}{\sqrt{2\pi T}} e^{-\frac{r_0^2}{4T}} \sum_{n=1,3,\ldots}^{\infty} \frac{1}{n} \sin\left(\frac{n\pi\theta_0}{\alpha}\right) \\
* \left[I_{\frac{1}{2}\left(\frac{n\pi}{\alpha}+1\right)}\left(\frac{r_0^2}{4T}\right) + I_{\frac{1}{2}\left(\frac{n\pi}{\alpha}-1\right)}\left(\frac{r_0^2}{4T}\right) \right]
\end{aligned}
\tag{D13}
$$

where θ_0, r_0 and α are defined as in the general form.

Appendix E: Derivation of gradient w.r.t. trade parameters

We want to identify critical points (N^*, T^*) of the minimal expected execution cost function developed in the previous section. It is well known that for a continuous function a critical point is any point (N^*, T^*) for which the gradient

$\nabla c^*(N,T) = \left(\frac{\partial c^*}{\partial N}, \frac{\partial c^*}{\partial T}\right)^\top$ evaluates to the zero vector. Thus, we are looking for the solution to $\nabla c^*(N^*,T^*) = (0,0)^\top$ or

$$\nabla c^*(N^*,T^*) = \begin{pmatrix} (\eta - bv) - \frac{\lambda(N^*,T^*)}{2h(T^*)} \\ \frac{\lambda(N^*,T^*)}{4bh(T^*)^2}\left(\lambda(N^*,T^*)h'(T^*) - 2ag'(T^*)h(T^*)\right) \end{pmatrix} = \begin{pmatrix} 0 \\ 0 \end{pmatrix} \quad \text{(E14)}$$

, where $\lambda(N,T) = Nb + ag(T)$. The problem of finding the critical points $(N^*,T^*)^\top$ can be expressed as a system of two equations in two variables N^* and T^*

$$(\eta - bv) - \frac{\lambda(N^*,T^*)}{2h(T^*)} = 0 \quad \text{(E15a)}$$

$$\frac{\lambda(N^*,T^*)}{4bh(T^*)^2}\left(\lambda(N^*,T^*)h'(T^*) - 2ag'(T^*)h(T^*)\right) = 0 \quad \text{(E15b)}$$

Because λ is strictly positive the second equation can be simplified and we can write

$$(\eta - bv) - \frac{\lambda(N^*,T^*)}{2h(T^*)} = 0 \quad \text{(E16a)}$$

$$\lambda(N^*,T^*)h'(T^*) - 2ag'(T^*)h(T^*) = 0 \quad \text{(E16b)}$$

Solving both expressions for N^* and combining the two equations results in a single equation in variable T^*

$$\begin{aligned} \frac{1}{b}(2h(T^*)(\eta - bv) - ag(T^*)) &= \frac{2ag'(T^*)h(T^*)}{bh'(T^*)} - \frac{a}{b}g(T^*) \\ h'(T^*)(\eta - bv) &= ag'(T^*) \\ \frac{h'(T^*)}{g'(T^*)} &= \frac{a}{\eta - bv}. \end{aligned} \quad \text{(E17)}$$

In order to further simplify this equation we separate the nested sum term in $h(T)$ into two independent sums as follows

$$\begin{aligned} &\sum_{j=1}^{J}\left(\sum_{i=j}^{J} P_i(T)K_i\right)P_j(T)K_j \\ &= \begin{cases} (P_1(T))^2 & \text{if} \quad J = 1 \\ \sum_{j=1}^{J}(P_j(T)K_j)^2 + \sum_{j=1}^{J-1} P_j(T)K_j \sum_{i=j+1}^{J} P_i(T)K_i & \text{else} \end{cases} \end{aligned} \quad \text{(E18)}$$

Note that we have made use of the fact that $K_1 = 1$ if $J = 1$ and thus this special case results in a very simple expression. Therewith, the derivative $h'(T^*)$ evaluates to

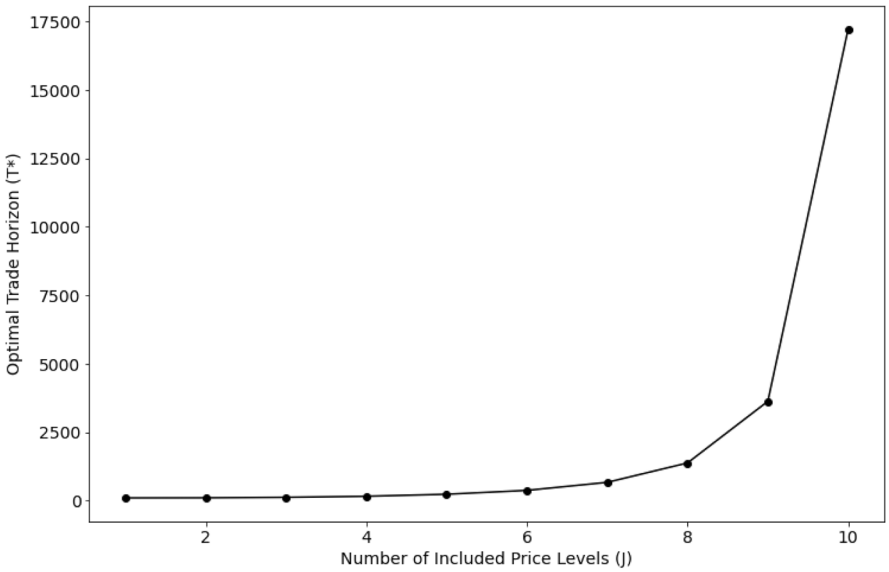


Fig. 11 Optimal trade period T^* in seconds (y-axis) for different number of LOB price levels included in the execution strategy

$$h'(T^*) = \begin{cases} -g'(T^*) + 2P_1'(T)P_1(T)K_1 & \text{if} \quad J = 1 \\ -g'(T^*) + 2\sum_{j=1}^{J} P_j'(T)P_j(T)K_j + \sum_{j=1}^{J-1} P_j'(T)K_j \sum_{i=j+1}^{J} P_i'(T)K_i & \text{else} \end{cases} \tag{E19}$$

As a result, for the case where $J = 1$ the following solution can easily be derived $T^* = P_1^{-1}\left(\frac{\eta - bv + a}{2(\eta - bv)}\right)$. On the other hand, the general case where $J > 1$ involves the probability density functions $P_j'(T^*) = \phi_j(T^*)$ and thus becomes analytically intractable. However, we are able to reformulate Eq. (E17) as a root-finding problem

$$2\sum_{j=1}^{J} \phi_j(T^*)P_j(T^*)K_j + \sum_{j=1}^{J-1} \phi_j(T^*)K_j \sum_{i=j+1}^{J} \phi_i(T^*)K_i - \zeta \sum_{j=1}^{J} \phi_j(T^*)K_j = 0 \tag{E20}$$

with constant $\zeta = \frac{a}{\eta - bv} + 1$. Thus, we are able to numerically solve for T^*. To better understand this relationship we compute and plot the criticaltrade period T^* for an increasing number of active price levels J. Doing this again for the same LOB snapshot 2021-05-04T18:00:00 and the exponential kernel yields the following graph.

From Fig. 11, it is clear that T^* increases exponentially when more price levels are included in the trading strategy, which suggests that $T^* \to \infty$ as J grows larger. This coincides with the intuition that the larger trade period leads to higher

execution probabilities $P_j(T^*)$ and thus to more trade volume being, in expectation, executed as limit orders at various price levels. Because these limit orders accrue volume rebate and maker rebate the minimal cost is expected to decrease.

Appendix F: Derivation of gradient w.r.t. exchange parameters

We want to identify critical points (a^*, b^*) of the minimal execution cost function shown in Eq. (C11). Similarly to the approach taken in Sect. E we find the critical points as any point (a, b) for which the gradient $\nabla c^*_{N,T}(a,b) = \left(\frac{\partial c^*_{N,T}}{\partial a}, \frac{\partial c^*_{N,T}}{\partial b}\right)^\top$ evaluates to the zero vector. In other words, we are looking for the solution to $\nabla c^*_{N,T}(a^*, b^*) = (0,0)^\top$ or

$$\nabla c^*_{N,T}(a^*, b^*) = -\begin{pmatrix} \frac{g(T)}{2h(T)}\left(N + g(T)\frac{a^*}{b^*}\right) \\ \frac{1}{4h(T)}\left(4vh(T)N + N^2 + g(T)^2\frac{(a^*)^2}{(b^*)^2}\right) \end{pmatrix} = \begin{pmatrix} 0 \\ 0 \end{pmatrix} \tag{F21}$$

Thus, finding the critical points $(a^*, b^*)^\top$ corresponds to solving the following system of equations

$$-\frac{g(T)}{2h(T)}\left(N + g(T)\frac{a^*}{b^*}\right) = 0 \tag{F22a}$$

$$-\frac{1}{4h(T)}\left(4vh(T)N + N^2 + g(T)^2\frac{(a^*)^2}{(b^*)^2}\right) = 0. \tag{F22b}$$

We can further simplify these equations

$$N + g(T)\frac{a^*}{b^*} = 0 \tag{F23a}$$

$$4vh(T)N + N^2 + g(T)^2\frac{(a^*)^2}{(b^*)^2} = 0. \tag{F23b}$$

Because in both equations all the terms are strictly positive we conclude that no result exists for this system. Thus, the minimal expected execution cost function in fee rebates a and b does not have a critical point $(a^*, b^*)^\top$ and, as a result, also no min-min or min-max.

Author contributions All authors have contributed equally to this work.

Funding Open access funding provided by ZHAW Zurich University of Applied Sciences. No funding was received to assist with the preparation of this manuscript.

Data availability The data used in the preparation of this manuscript are available from the Kraken Exchange Public API at https://docs.kraken.com/rest/.

Code availability The code generated in the preparation of this manuscript is available from the authors upon reasonable request.

Declarations

Conflict of interest The authors have no relevant financial or non-financial interests to disclose.

Ethics approval Not applicable

Consent to participate Not applicable

Consent for publication Not applicable

Open Access This article is licensed under a Creative Commons Attribution 4.0 International License, which permits use, sharing, adaptation, distribution and reproduction in any medium or format, as long as you give appropriate credit to the original author(s) and the source, provide a link to the Creative Commons licence, and indicate if changes were made. The images or other third party material in this article are included in the article's Creative Commons licence, unless indicated otherwise in a credit line to the material. If material is not included in the article's Creative Commons licence and your intended use is not permitted by statutory regulation or exceeds the permitted use, you will need to obtain permission directly from the copyright holder. To view a copy of this licence, visit http://creativecommons.org/licenses/by/4.0/.

References

Alfonsi, A., Fruth, A., & Schied, A. (2010). Optimal execution strategies in limit order books with general shape functions. *Quantitative Finance, 10*(2), 143–157. https://doi.org/10.1080/14697680802595700

Almgren, R., & Chriss, N. (2000). Optimal execution of portfolio transactions. *Journal of Risk, 3*(2), 5–39. https://doi.org/10.21314/JOR.2001.041

Almgren, R. F. (2003). Optimal execution with nonlinear impact functions and trading enhanced risk. *Applied Mathematical Finance, 10*(1), 1–18. https://doi.org/10.1080/135048602100056

Battalio, R., Corwin, S. A., & Jennings, R. (2016). Can brokers have it all? On the relation between make-take fees and limit order execution quality. *The Journal of Finance, 71*(5), 2193–2238. https://doi.org/10.1111/jofi.12422

Ben-Rephael, A., & Israelsen, R. D. (2017). Are some clients more equal than others? An analysis of asset management companies' execution costs. *Review of Finance, 22*(5), 1705–1736. https://doi.org/10.1093/rof/rfx043

Bertsimas, D., & Lo, A. W. (1998). Optimal control of execution costs. *Journal of Financial Markets, 1*(1), 1–50. https://doi.org/10.1016/S1386-4181(97)00012-8

Black, J. R. (2022). The impact of make-take fees on market efficiency. *Review of Quantitative Finance and Accounting, 58*(3), 1015–1035. https://doi.org/10.1007/s11156-021-01016

Brauneis, A., Mestel, R., Riordan, R., & Theissen, E. (2022). The anatomy of a fee change—Evidence from cryptocurrency markets. *Journal of Empirical Finance, 67*, 152–167. https://doi.org/10.1016/j.jempfin.2022.03.003

Brown, D. B., & Smith, J. E. (2011). Dynamic portfolio optimization with transaction costs: Heuristics and dual bounds. *Management Science, 57*(10), 1752–1770. https://doi.org/10.1287/mnsc.1110.1377

Buy BitcoinWorldwide (2021). Bitcoin treasuries. https://www.buybitcoinworldwide.com/treasuries/. Accessed 31 Dec 2021.

Chen, N., Kou, S., & Wang, C. (2018). A partitioning algorithm for Markov decision processes with applications to market microstructure. *Management Science, 64*(2), 784–803. https://doi.org/10.1287/mnsc.2016.2639

Cheng, X., Giacinto, M. D., & Wang, T.-H. (2017). Optimal execution with uncertain order fills in Almgren–Chriss framework. *Quantitative Finance, 17*(1), 55–69. https://doi.org/10.1080/14697688.2016.1185531

Cho, J.-W., & Nelling, E. (2000). The probability of limit-order execution. *Financial Analysts Journal, 56*(5), 28–33. https://doi.org/10.2469/faj.v56.n5.2387

Cimon, D. A. (2021). Broker routing decisions in limit order markets. *Journal of Financial Markets, 54*, 100602. https://doi.org/10.1016/j.finmar.2020.100602

Colliard, J.-E., & Foucault, T. (2012). Trading fees and efficiency in limit order markets. *The Review of Financial Studies, 25*(11), 3389–3421. https://doi.org/10.1093/rfs/hhs089

Cont, R., & Kukanov, A. (2017). Optimal order placement in limit order markets. *Quantitative Finance, 17*(1), 21–39. https://doi.org/10.1080/14697688.2016.1190030

Edelen, R., Evans, R., & Kadlec, G. (2013). Shedding light on "invisible'' costs: Trading costs and mutual fund performance. *Financial Analysts Journal, 69*(1), 33–44. https://doi.org/10.2469/faj.v69.n1.6

Euch, O. E., Mastrolia, T., Rosenbaum, M., & Touzi, N. (2021). Optimal make-take fees for market making regulation. *Mathematical Finance, 31*(1), 109–148. https://doi.org/10.1111/mafi.12295

Figueroa-Lopez, J. E., Lee, H., & Pasupathy, R. (2018). Optimal placement of a small order in a diffusive limit order book. *High Frequency, 1*(2), 87–116. https://doi.org/10.1002/hf2.10017

Foley, S., Krekel, W., Mollica, V., & Svec, J. (2023). Not so fast: Identifying and remediating slow and imprecise cryptocurrency exchange data. *Finance Research Letters, 51*, 103401. https://doi.org/10.1016/j.frl.2022.103401

Forsyth, P. (2011). A Hamilton Jacobi bellman approach to optimal trade execution. *Applied Numerical Mathematics, 61*, 241–265. https://doi.org/10.1016/j.apnum.2010.10.004

Forsyth, P., Kennedy, J., Tse, S., & Windcliff, H. (2009). Optimal trade execution: A mean quadratic variation approach. *Journal of Economic Dynamics and Control, 36*, 1971–1991. https://doi.org/10.1016/j.jedc.2012.05.007

Gatheral, J., & Schied, A. (2012). Optimal trade execution under geometric Brownian motion in the Almgren and Chriss framework. *International Journal of Theoretical and Applied Finance (IJTAF), 14*, 353–368. https://doi.org/10.1142/S0219024911006577

Guant, O., Lehalle, C.-A., & Fernandez-Tapia, J. (2012). Optimal portfolio liquidation with limit orders. *SIAM Journal on Financial Mathematics, 3*(1), 740–764. https://doi.org/10.1137/110850475

Guo, X., de Larrard, A., & Ruan, Z. (2017). Optimal placement in a limit order book: An analytical approach. *Mathematics and Financial Economics, 11*, 189–213. https://doi.org/10.1007/s11579-016-0177-5

Huitema, R. (2014). Optimal portfolio execution using market and limit orders. *SSRN Electronic Journal*. https://doi.org/10.2139/ssrn.1977553

Jalal, R.N.-U.-D., Alon, I., & Paltrinieri, A. (2021). A bibliometric review of cryptocurrencies as a financial asset. *Technology Analysis and Strategic Management*. https://doi.org/10.1080/09537325.2021.1939001

Kashyap, R. (2020). David vs goliath (you against the markets), a dynamic programming approach to separate the impact and timing of trading costs. *Physica A: Statistical Mechanics and its Applications, 545*, 122848. https://doi.org/10.1016/j.physa.2019.122848

Kirchner, M., & Vetter, S. (2020). Hawkes model specification for limit order books. *The European Journal of Finance*. https://doi.org/10.1080/1351847X.2020.1784974

Kozhan, R., & Tham, W. W. (2012). Execution risk in high-frequency arbitrage. *Management Science, 58*(11), 2131–2149. https://doi.org/10.1287/mnsc.1120.1541

Kraken (2021). Kraken fee schedule. https://www.kraken.com/en-us/features/fee-schedule. Accessed 15 Dec 2021.

Lin, Y., Swan, P. L., & Harris, F. R. H. D. (2019). Why maker-taker fees improve exchange quality: Theory and natural experimental evidence. *SSRN Electronic Journal*. https://doi.org/10.2139/ssrn.3034901

Lo, A. W., MacKinlay, A., & Zhang, J. (2002). Econometric models of limit-order executions. *Journal of Financial Economics, 65*(1), 31–71. https://doi.org/10.1016/S0304-405X(02)00134-4

Obizhaeva, A. A., & Wang, J. (2013). Optimal trading strategy and supply/demand dynamics. *Journal of Financial Markets, 16*(1), 1–32. https://doi.org/10.1016/j.finmar.2012.09.001

Omura, K., Tanigawa, Y., & Uno, J. (2000). Execution probability of limit orders on the Tokyo stock exchange. *SSRN Electronic Journal*. https://doi.org/10.2139/ssrn.252588

Panayides, M. A., Rindi, B., & Werner, I. M. (2017). Trading fees and intermarket competition. *SSRN Electronic Journal*. https://doi.org/10.2139/ssrn.2954512 (BAFFI CAREFIN Centre Research Paper No. 2017-51, Proceedings of Paris December 2020 Finance Meeting EUROFIDAI—ESSEC).

Perold, A. F. (1988). The implementation shortfall. *The Journal of Portfolio Management, 14*(3), 4–9. https://doi.org/10.3905/jpm.1988.409150

Schnaubelt, M. (2021). Deep reinforcement learning for the optimal placement of cryptocurrency limit orders. *European Journal of Operational Research, 296*, 993–1006. https://doi.org/10.1016/j.ejor.2021.04.050

Siu, C. C., Guo, I., Zhu, S.-P., & Elliott, R. J. (2019). Optimal execution with regime switching market resilience. *Journal of Economic Dynamics and Control, 101*, 17–40. https://doi.org/10.1016/j.jedc.2019.01.006

Tsoukalas, G., Wang, J., & Giesecke, K. (2019). Dynamic portfolio execution. *Management Science, 65*(5), 2015–2040. https://doi.org/10.1287/mnsc.2017.2865

Yura, Y., Takayasu, H., Sornette, D., & Takayasu, M. (2014). Financial Brownian particle in the layered order-book fluid and fluctuation-dissipation relations. *Physical Review Letters, 112*, 098703. https://doi.org/10.1103/PhysRevLett.112.098703

Zhou, C. (2001). An analysis of default correlations and multiple defaults. *The Review of Financial Studies, 14*(2), 555–576. https://doi.org/10.1093/rfs/14.2.555

Publisher's Note Springer Nature remains neutral with regard to jurisdictional claims in published maps and institutional affiliations.